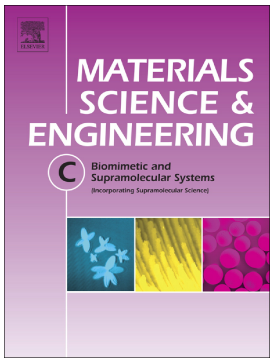

Highly porous novel chondro-instructive bioactive glass scaffolds tailored for cartilage tissue engineering

Clemens Gögele, Sven Wiltzsch, Armin Lenhart, Aurelio Civilleri, Thomas Martin Weiger, Kerstin Schäfer-Eckart, Bernd Minnich, Lukas Forchheimer, Markus Hornfeck, Gundula Schulze-Tanzil

PII: S0928-4931(21)00561-0

DOI: https://doi.org/10.1016/j.msec.2021.112421

Reference: MSC 112421

To appear in: *Materials Science & Engineering C*

Received date: 19 April 2021

Revised date: 23 August 2021

Accepted date: 6 September 2021

Please cite this article as: C. Gögele, S. Wiltzsch, A. Lenhart, et al., Highly porous novel chondro-instructive bioactive glass scaffolds tailored for cartilage tissue engineering, *Materials Science & Engineering C* (2021), https://doi.org/10.1016/j.msec.2021.112421

Highly porous novel chondro-instructive bioactive glass scaffolds tailored for cartilage tissue engineering

Clemens Gögele[1,2], Sven Wiltzsch[3], Armin Lenhart[3], Aurelio Civilleri[1,4], Thomas Martin Weiger[2], Kerstin Schäfer-Eckart[5], Bernd Minnich[2], Lukas Forchheimer[3], Markus Hornfeck[3], Gundula Schulze-Tanzil[1*]

[1] Institute of Anatomy and Cell Biology, Paracelsus Medical University, Nuremberg and Salzburg, Prof. Ernst-Nathan Str. 1, 90419 Nuremberg, Germany, clemens.goegele@pmu.ac.at, gundula.schulze@pmu.ac.at
[2] Department of Biosciences, Paris Lodron University Salzburg, Hellbrunnerstraße 34, 5020 Salzburg, Austria, clemens.goegele@pmu.ac.at, thomas.weiger@sbg.ac.at, bernd.minnich@sbg.ac.at
[3] Faculty of Material Engineering, Nuremberg, Institute of Technology Georg Simon Ohm, Nuremberg, Germany, sven.wiltzsch@th-nuernberg.de, armin.lenhart@th-nuernberg.de, lforchheimer@web.de, markus.hornfeck@th-nuernberg.de
[4] Department of Civil, Environmental, Aerospace, Materials Engineering Universita' di Palermo, Palermo, Italy, aurelio.civilleri@community.unipa.it
[5] Bone marrow Transplantation Unit, Medizinische Klinik 5, Klinikum Nürnberg, Paracelsus Medizinische Privatuniversität, Nuremberg, Germany, kerstin.schaefer-eckart@klinikum-nuernberg.de

***Corresponding author**
Univ. Prof. Dr. Gundula Schulze-Tanzil
Institute of Anatomy and Cell Biology
Paracelsus Medical University
Prof. Ernst Nathan Str.1
Nuremberg, Germany, 90419, Bavaria
Tel: +49-911-398-(11) 6772
Fax: +49-911-398-6774
E-Mail: gundula@schulze@pmu.ac.at

Abstract

Cartilage injuries remain challenging since the regenerative capacity of cartilage is extremely low. The aim was to design a novel type of bioactive glass (BG) scaffold with suitable topology that allows the formation of cartilage-specific extracellular matrix (ECM) after colonization with chondrogenic cells for cartilage repair. Highly porous scaffolds with interconnecting pores consisting of 100% BG were manufactured using a melting, milling, sintering and leaching technique. Scaffolds were colonized with porcine articular chondrocytes (pAC) and undifferentiated human mesenchymal stromal cells (hMSC) for up to 35 days.

Scaffolds displayed high cytocompatibility with no major pH shift. Scanning electron microscopy revealed the intimate pAC-scaffold interaction with typical cell morphology. After 14 days MSCs formed cell clusters but still expressed cartilage markers. Both cell types showed aggrecan, SOX9 gene and protein expression, cartilage proteoglycan and sulfated glycosaminoglycan synthesis for the whole culture time. Despite type II collagen gene expression could not anymore be detected at day 35, protein synthesis was visualized for

both cell types during the whole culturing period, increasing in pAC and declining after day 14 in hMSC cultures.

The novel BG scaffold was stable, cytocompatible and cartilage-specific protein synthesis indicated maintenance of pAC´s differentiated phenotype and chondro-instructive effects on hMSCs.

Key words: bioactive glass, cartilage, articular chondrocytes, human mesenchymal stromal cells, type II collagen

Short title: bioactive glass for cartilage tissue engineering

Highlights

- a novel bioactive glass (Car12N) tailored for cartilage tissue engineering (TE)
- Car12N induces no hydroxyapatite and pH shift
- highly porous 100% Car12N scaffolds have a topology suitable for cartilage TE
- Car12N is cytocompatible, allows cell adherence and chondrocytic phenotype maintenance.
- Car12N exerts some chondro-instructive effects on undifferentiated MSCs.

Abbreviation list

2D	two dimensional
3D	three dimensional
ACAN	gene coding for aggrecan
ACI	autologous chondrocyte implantation
ACTB	gene coding for beta-actin
BG	bioactive glass
BMSC	bone marrow derived mesenchymal stromal cells
CLSM	confocal laser scanning microscope
COL1A1	gene coding for type I collagen
COL2A1	gene coding for type II collagen
DAPI	4',6-diamidino-2-phenylindole
DMEM	Dulbecco's Modified Eagle's Medium
DMMB	dimethylmethylene blue

DMSO	dimethyl sulfoxide solution
ECM	extracellular matrix
EDTA	Ethylenediaminetetraacetic acid
ETOH	ethanol
FCS	fetal calf serum
FDA	fluorescein diacetate
HBSS	Hank's Balanced Salt Solution
HCl	hydrochloric acid
hMSC	human mesenchymal stromal cell
MACI	matrix assisted chondrocyte implantation
MTS	3-(4,5-dimethylthiazol-2-yl)-5-(3-carboxymethoxyphenyl)-2-(4-sulfophenyl)-2H-tetrazolium, inner salt
OA	osteoarthritis
pAC	porcine articular chondrocyte
PBS	phosphate buffered saline
PCL	polycaprolactone
PEG	poly(ethylene glycol)
PFA	paraformaldehyde
PG	proteoglycans
PI	propidium iodide
PL	platelet lysate
PLLA	Poly-L-lactic acid
PU	polyurethane
RT	room temperature
SD	standard deviation
SEM	scanning electron microscopy
sGAG	sulfated glycosaminoglycans
SI	silicon
SOX9	*SRY* (sex-determining region Y)*-box 9* protein
TBS	TRIS buffered saline
TE buffer	TRIS EDTA buffer

Highlights

- a novel bioactive glass (Car12N) tailored for cartilage tissue engineering (TE)

- Car12N induces no hydroxyapatite and pH shift
- highly porous 100 % Car12N scaffolds have a topology suitable for cartilage TE
- Car12N is cytocompatible, allows cell adherence and maintains chondrocytic phenotype.
- Car12N exerts some chondro-instructive effects on undifferentiated MSCs.

1. Introduction

Hyaline cartilage consists mainly of extracellular matrix (ECM), which is formed by few chondrocytes and contains neither nerves nor blood or lymphatic vessels. Therefore, chondrocytes can only be supplied by diffusion [1]. Cartilage injuries lead to cartilage ECM damages mainly of the type II collagen fibers, proteoglycans (PG), especially of the large PG aggrecan and sulfated glycosaminoglycans (sGAG) and a loss of chondrocytes [2]. The result is a reduction of the unique viscoelasticity of joint cartilage, an impairment in the gliding ability of the joint bodies and consequently, a high risk of developing osteoarthritis (OA) [3, 4]. Untreated OA progresses steadily and is accompanied by joint inflammation that affects not only the joint capsule, subchondral bone, surrounding ligaments, but also the intra-articular fat pad and results finally in complete cartilage destruction [5, 6]. OA is so far incurable [7]. Therefore, the development of OA resulting from traumatic cartilage injuries should be prevented by treatment of cartilage defects using chondrogenic cells and chondro-instructive scaffolds to cover defects. To facilitate intrinsic cartilage repair the implantation of autologous chondrocytes (autologous chondrocyte implantation, ACI) amplified in culture and implanted into the defective area has been recommended since decades [8-10]. The ACI technique is based on autologous chondrocyte isolation from a small biopsy of articular cartilage taken from a non-load bearing joint area; the resulting chondrocytes are multiplied *in vitro* and then inserted into the cartilage defect covered by a patch of e.g. the periost [10-12]. The idea of the procedure is that the autologous chondrocytes will repair the damaged area and form a new layer of natural articular cartilage. Today, in addition to ACI [11], the so-called matrix-associated chondrocyte implantation (MACI) is more and more common [13]. MACI is an expansion technique in which the obtained autologous chondrocytes are seeded on a matrix that corresponds exactly to the size of the cartilage defect [14, 15]. The MACI method is considered a promising cell therapy [16]. Long-term clinical results indicate that MACI might be a suitable option for long-term cartilage repair [12, 17]. To improve the outcome of MACI, versatile chondro-instructive biomaterials are required that can be validated using tissue engineering strategies. Cartilage tissue engineering strives not only for the preservation of the cartilage-specific phenotype of chondrocytes and their ECM production, but also for the stable fitting and integration of an implant into the cartilage defect [18, 19] which can be mediated by scaffolds [20]. Because of their suitable mechanical

properties, low toxicity and predictable biodegradation, different synthetic materials such as polymers, Poly-L-Lactic acid (PLLA), polyglactin/polydioxanone, polycaprolactone (PCL), polyglycolide or poly(ethylene glycol) (PEG) have been investigated for cartilage tissue engineering [21-25]. Since synthetic polymers are not bioactive on their own, it is promising to combine them with other materials such as bioactive glasses or ceramics [26-29]. In general, bioactive materials have been defined as materials that induce specific biological activities at the tissue-material interface, undergo a surface modification and lead to biochemical reactions [30-32].

Bioactive glass or bioglass (BG) is suitable as a biomaterial not only because its composition and structure can be precisely modified and tuned, but also because it can release various bioactive and cell stimulatory ions during the leaching process. During this process the glass scaffold emits alkaline ions such as Na^+ that result in the formation of a silica gel layer on the glass surface due to hydrolysis and this mechanism could result in an unfavorable increase in pH. In addition, the release of alkaline earth metal ions such as Ca^{2+} leads to hydroxyapatite deposition in the presence of PO_4^{3-} [33]. A detailed list of the patented ion composition of well-known BGs is given in **Table 1** and compared with the novel BG addressed in the present study. The listed BG variations (BG1393 and BG45S5) and other variations of them have been specifically designed to stimulate bone healing [34-37]. They share the formation of hydroxyapatite. A strong interaction with the surrounding tissue and the activation of tissue-specific genes e.g. by hydroxyapatite are necessary for an effective bone reconstruction [38-40]. Hydroxyapatite is the main inorganic salt of bone and teeth, which is a calcium phosphate bioceramic [41, 42]. Moreover, although some authors were also able to show that a hydroxyapatite layer can support cartilage repair, proliferation and glycosaminoglycan (GAG) synthesis of chondrocytes, it remains the main component of the bone matrix and is not degradable [43-45]. Hence, this study aimed to find a novel BG composition which does not allow hydroxyapatite formation.

The ionic composition of a BG is the decisive factor not only for bioactivity but also for adapting the rate of BG degradation [46]. Silicon (Si) is the major component of BG. It could enhance proliferation and differentiation of progenitor cells [47]. Other ions like calcium (Ca^{2+}), strontium (Sr^{2+}), or magnesium (Mg^{2+}) are associated with osteogenic differentiation, progenitor cell growth and maintenance [48-51].

Due to the fact that pure bioactive glass scaffolds are brittle and cannot be well processed as well as withstand the mechanical loads in the body, they have to be additionally strengthened [52]. For the preparation of bioactive composites, polymers such as poly(L-lactic) (PLLA), poly(D,L-lactic acid) (PDLLA), polyethylene, poly(methyl methacrylate), polysulfones or collagens are used as a basis and then supplemented with BG/ ceramic particles, powders or fibers [53]. These compositions are not only suitable for bone tissue engineering [54], but

allow also to some degree cartilage tissue engineering [25]. However, cartilage tissue engineering could be facilitated in future by developing chondro-instructive BG species. The use of autologous chondrocytes for cartilage tissue engineering based approach for cartilage repair is limited by donor-site morbidity. In addition, the expansion of chondrocytes in cell culture is costly, time-consuming and leads to an irreversible phenotypic shift after prolonged culturing periods [55-57]. Precursor cells with high chondrogenic capacity such as bone-marrow derived mesenchymal stromal cells (BMSCs) provide an alternative because they can be harvested with very low risk of donor site morbidity and can be rapidly amplified to high numbers before chondrogenically differentiated, making scaffold colonization possible [58, 59].

The aim of this study was to characterize performance of chondrocytes and human mesenchymal stromal cells (hMSCs) on a highly porous pure BG scaffold named Car12N with a novel composition and suitable topology, particularly adapted for cartilage tissue engineering purposes with no risk of hydroxyapatite deposition due to lack of alkaline earth metal ions and pH shift. Hence, in this study, cell morphology, adherence, survival and cartilage ECM expression profiles were monitored in porcine articular chondrocytes (pACs) and hMSCs seeded on the Car12N scaffold to assess the influence of its bioactivity on chondrogenesis and tissue formation. MSCs are a potential regenerative cell source of the body and could also offer a significant benefit in terms of personalized cartilage defect regeneration. Furthermore, the question arises whether hMSCs can already pre-differentiate in the chondrogenic direction only by long-term cultivation on the BG scaffold.

2. Materials and Methods

2.1 Scaffold composition

Table 1 Detailed composition of the raw glass used for Car12N scaffold preparation [%]

Ions	Mass percentage	Putative effect on BG processing or cells
SiO_2	62.7	
P_2O_5	7	Network former
B_2O_3	2	Network changer
Na_2O	25.6	Boron-ions: might stimulate cell proliferation
K_2O	1	Stabilizing gel layer
TiO_2	0.12	Titanium-ions: might stimulate cell proliferation
ZrO_2	0.1	Zirconium-ions: anti-inflammatory
CuO	0.02	Copper-ions: antibacterial
ZnO	0.06	Zinc- and natrium-ions: might stimulate cell proliferation
NaCl	0.3	
NaF	0.2	
Na_2SO_4	0.4	Homogenizes melted mass
KNO_3	0.5	Optimization of melting

Table 2 Main components of our BG (Car12N red underlined) in comparison to other typical BG species like 1393, 45S5, 60S, 45S5F, 45S5.4F, 45S5B5 and 52S4.6. The values refer to the percentage of the glass [%].

BG	1393	45S5	60S	45S5F	45S5.4F	45S5B5	52S4.6	Car12N
SiO_2	53	45	60	45	45	40	52	62.7
P_2O_5	4	6	4.6	6	6	6	6	7
CaO	20	24.5	19.6	12.25	14.7	24.5	21	-
CaF_2	-	-	-	12.5	9.8	-	-	-
Na_2O	6	24.5	17.7	24.5	24.5	24.5	21	28
B_2O_3	-	-	-	-	-	5	-	2

2.2 Scaffold preparation

For the production of the BG scaffold (Car12N) a recently patented glass composition (Car12N) was used (DE 10 2018 114 946 B3, 2019) **(Table 1)**. The chemical components **(Table 2)** were mixed and combined to melt a raw glass body, which was then crushed and ground in a ball mill. The glass powder obtained (grain size < 40 µm) was suspended with an aqueous solvent (isopropanol, Carl Roth GmbH, Karlsruhe, Germany) and applied to a porous polyurethane sponge (Eurofoam Deutschland GmbH Schaumstoffe, Wiesbaden, Germany). The powder particles adhered evenly to the surface of the sponge, thus reproducing the sponge geometry. A subsequent 2 hours (h) heat treatment (600-740°C)

completely decomposed the polyurethane sponge and sintered the glass particles together forming a highly porous scaffold. In the last step, a leaching process of 6 days with 0.1 M HCl at room temperature (RT) was performed to reduce its alkali content. Scaffolds were stored in sterile, hypotonic and pyrogen free water (Carl Roth GmbH) **(Fig. 1)**.

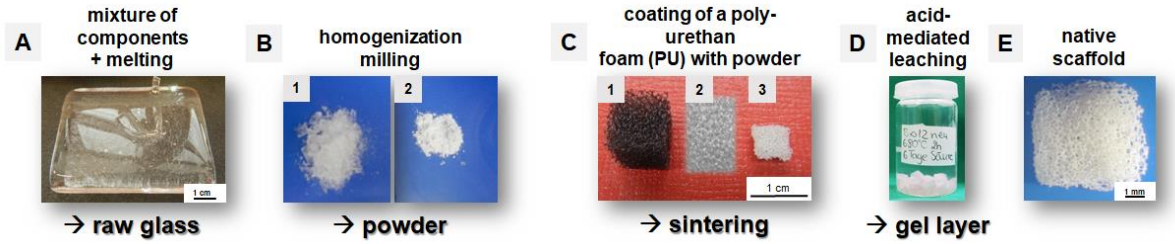

Figure 1 ***Scaffold preparation process****. Raw glass is fabricated by mixing and melting of the components* ***(A)****. The glass body was crushed to powder of defined particle sizes (****B****, roughly 1 and fine 2). The poly-urethane foam (PU) (1) is coated with powder (2) which is sintered to a scaffold by high temperature (3)****(C)****. HCl treatment leads to a leaching process which results in gel layer formation at the surface of the scaffold* ***(D)****. Macroscopical view on the scaffold* ***(E)****. Scale bars: 1 cm.*

2.3 Isolation of porcine articular chondrocytes

PACs were isolated from 7 healthy knee joints from 4-6 month old pigs derived from the abattoir. The harvested cartilage pieces were cut into small slices (2 mm) and digested by collagenase NB5 derived from *Clostridium histolyticum* (1 mg/mL, Merck KGaA, Darmstadt, Germany) in chondrocyte growth medium (96% [v/v] DMEM/Ham's F-12 [1:1] with stable L-glutamin, 1% [v/v] amphotericin B, 1% [v/v] MEM amino acids, 1% [v/v] penicillin/streptomycin, 1% [v/v] ascorbic acid supplemented with 10% fetal calf serum [FCS] (all products from Bio&Sell, Feucht, Germany) overnight in a rotatory device at 37°C. After sieving and washing, isolated chondrocytes were cultured in chondrocyte growth medium in T175 flask (CellPlus, Sarstedt AG, Nümbrecht, Germany). For expansion, chondrocytes were detached with 0.05%/0.02% trypsin/ Ethylenediaminetetraacetic acid (EDTA) solution (Bio&Sell) and seeded in T175 flasks. Growth medium changes were done every second day.

2.4 Isolation of human mesenchymal stromal cells

Donors of hMSCs were males (n=15) and females (n=6) with an average age of 28 ± 8.5 who were voluntary bone marrow donors. Harvesting human tissue samples for hMSCs isolation was approved by ethical commission of the Bavarian medical association (no. 17074, 6th February 2018) for experiments with human derived tissues. It was in accordance with the declaration of Helsinki. Bone marrow blood was obtained by iliac crest biopsies from the bone marrow transplantation unit of the Nuremberg General Hospital. Freshly harvested bone marrow blood was mixed with MSC growth medium (1:4) and pipetted into a T175 flask (Sarstedt). The growth medium consisted of Dulbecco´s modified Eagle´s medium (DMEM

with stable glutamine [3.7 g/L $NaHCO_3$ and 4.5 g/L D-glucose], BioSell), 5% human growth factor-rich human Platelet Lysate (PL) solution (PL BioScience, Aachen, Germany), 0.04% heparin (PL BioScience), 1% [v/v] amphotericin B, 1% natrium pyruvate (Biochrom, Berlin, Germany), 1% penicillin/streptomycin (Bio&Sell). After three days, 10 mL fresh medium were added to each flask and after three additional days the medium was completely removed. Adherent cells were washed twice with phosphate buffered saline (PBS) and incubated with 20 mL fresh medium until a confluency of 80 - 90% was reached. For phenotype characterization of undifferentiated hMSCs, immunocytochemical staining was performed. For this step, 1.8 x 10^4 hMSCs per cm^2 were seeded on a glass cover slip. After 48 h cultivation time, the samples were prepared for immunocytochemical staining (description of the further steps for immunocytochemical staining is listed below see 2.13).

2.5 Cytotoxicity assay

The murine fibroblast cell line L929 (derived from subcutaneous tissue, strain C3H/An, from Cell Line Services, Germany) was used for biological evaluation of cytotoxicity according to the national standard DIN EN ISO 10993-5 2009-10 norm. Thawed primary pACs, hMSCs (both derived from three different donors) and L929 cells were seeded with an initial density of 1.0 x 10^4 cells/cm^2 in cell culture flasks and cultured in growth medium until 80–90% confluence at 37°C and 5% CO_2 was reached. Growth medium was changed three times a week. Extracts from three different scaffold charges were prepared to determine potential cytotoxic effects. Cell-specific growth medium was used as extraction medium. The BG scaffolds were sterilized with 0.1 M HCl solution and washed three times for 10 min with sterile aqua dest. to get rid of the HCl. Six scaffolds (0.199 g) were incubated in 1 mL extraction medium at 37°C and 5% CO_2 for 48 h under aseptic conditions using sterile, chemically inert cell culture plates. Cells (L929, pACs, hMSCs) were seeded in 96-well cell plates (Sarstedt) with an initial density of 1.0 x 10^4 cells/cm^2 and the cells were incubated for 24 h at 37 °C and 5% CO_2 to allow cell adherence. The growth medium was removed and the cells were cultured with 100 µL extraction or control solutions per well for 24 h 37°C and 5% CO_2. A 10% dimethyl sulfoxide solution (DMSO, Carl Roth GmbH) was prepared with growth medium and used as a positive control. Pure growth medium was applied as negative control. After 24 h of incubation with the respective extracts, the medium was completely discarded. 80 µL growth medium and 20 µL [3-(4,5-dimethylthiazol-2-yl)-5-(3-carboxymethoxyphenyl)-2-(4-sulfophenyl)-2H-tetrazolium, inner salt; MTS] solution (CellTiter 96®Aqueous One Solution Cell Proliferation Assay, Promega GmbH, Walldorf, Germany) were added to each well. The cells were incubated for an additional 2 h under standard culture conditions and absorbance was measured photometrically at a wavelength of 490 nm (Tecan Austria GmbH, Grödig, Austria).

2.6 pH measurement

The pH of the pure growth medium (10 mL), of uncolonized scaffolds (6 scaffolds in 10 mL culture medium) and pAC colonized scaffolds (6 scaffolds in 10 mL growth medium) was measured at RT with a pH meter (PCE-PH20S, PCE Americas Inc., Florida, USA).

2.7 Scaffold colonization

Cubic scaffolds with a length/width of 3.0 ± 0.5 mm (18 mm^3) and between 1 - 2 mm in height were sterilized in 0.1 M HCl solution for five days after production. The scaffolds were washed three times with purified poor endotoxin water and stored in water until colonization. Before colonization scaffold were transferred in a TubeSpin bioreactor tube (TPP, Trasadingen, Switzerland) and pre-incubated for 1 h in FCS. $5 x 10^5$ primary cells (27.778 cells/mm^3) pACs or hMSCs) per scaffold were used for dynamic seeding in 5 mL cartilage or stem cell growth medium. Using a rotatory device (Bartelt GmbH, Graz, Austria) with 36 rpm at 37°C guaranteed a homogenous distribution of the cells on the scaffold. Medium changes were executed every second day until the cultivation was stopped at day 7, 14, 21, 28 and 35. Three independent experiments with cells isolated from three different donors were performed.

2.8 Vitality assay

To check if cells were alive or dead, a live/dead staining was performed with 1 µL propidium iodide (PI, 1% stock solution in A. dest., Thermo Fisher Scientific, Darmstadt, Germany) and 5 µL fluorescein diacetate (FDA, stock solution: 3 mg mL^{-1} in acetone, Sigma-Aldrich) in 1 mL PBS. Cell vitality was determined after 7, 14, 21, 28 and 35 days. For performing the live/dead staining, the scaffolds were removed from growth medium, 50 µL of stain solution was added and transferred to a microscopic cover slide. After a 5 min incubation period at RT, the fluorescence of live and dead cells was monitored using a Leica SPEII DMi8 confocal laser scanning microscope (CLSM, Leica, Wetzlar, Germany). Based on the vitality assay, three different pictures with vital and dead cells from three independent experiments were evaluated. The pictures were “split” with the ImageJ 1.48v software in the green and red channel. The amount of vital (green) and dead (red) cells on the scaffold surface was calculated with the “particles analyzer” feature in the program. For the calculation of the vitality per scaffold surface, the amount of vital (green) and dead (red) cells were evaluated. The percentage of vitality refers to the sum of green and red dots. For determining the “colonized scaffold surface” only the green channel was taken and the area of vital cells was chosen.

2.9 SEM analysis

Scaffolds were first fixed in 2% paraformaldehyde (PFA), 2.5% glutaraldehyde (Carl Roth GmbH) in PBS without Ca^{2+} and Mg^{2+} overnight at 4°C, washed in PBS four times for 15 min and fixed in 1% osmium tetroxide (OsO_4). Afterwards, the scaffolds were gently rinsed four times á 15 min in PBS and dehydrated in an ascending ethanol (ETOH) series (70%, 80%, 90% and 96% ETOH each 30 min) and three times 100% ETOH á 15 min. Then, the samples were critical point dried, mounted onto specimen stubs and sputtered (agar auto carbon coater, Agar scientific Ltd, Essex, UK) with a thin layer of carbon (≈13 nm) before SEM images were taken under an ESEM XL30 (FEI Europe B.V., Eindhoven, NL) at an accelerating voltage of 20 kV.

2.10 Measurement of total DNA and GAG content

By CyQUANT® NF Cell Proliferation Assay the influence of respective treatment on cell division was examined after 7, 14, 21, 28 and 35 days. The standard curve was generated by serial dilution of calf thymus DNA stock solution (1 mg mL^{-1}) with TE-buffer (TRIS EDTA buffer, 10 mM TRIS [pH 8.0], 1 mM EDTA in Aqua dest.). For the standard curve, 25 µL of the serial calf thymus DNA dilution was mixed with 25 µL of CyQuant dye solution (1x Hank's Balanced Salt Solution [HBSS] + dye binding solution 1:250 [ThermoFisher Scientific Inc., Waltham, USA]). After analyzing time points (7, 14, 21, 28 and 35 days) of 3D long term culture, scaffolds were transferred to RNase and DNase free 2 ml safe seal tubes (Sarstedt) with 50 µl of the Proteinase K digestion buffer (50 mM TRIS/HCl, 1 mM EDTA, 0.5% Tween 20) containing 0.5 mg mL^{-1} proteinase K (PanReac, ApplyChem, Darmstadt, Germany). Samples were homogenized with a 7 mm stainless steel bead (RNase and DNase free, sterile, Qiagen, Hilden, Germany) by using the Tissue Lyser (Qiagen, 50 Hz, 5 min, RT). Then, 250 µL of the proteinase K digestion buffer containing 0.5 mg mL-1 proteinase K was added. All samples were digested for 16 h at 56°C under continuous shaking. The enzymatic reaction was stopped by freezing the samples at -20°C for 30 min. Before DNA quantification, all samples were thawed and then centrifuged for 15 min at 16483.55 g. 10 µL of each sample was added to 150 µL TE buffer and thoroughly mixed. Samples were transferred in triplicate with 25 µL of the sample dilution to a black, flat bottom 96-well plate (Brand GmbH, Wertheim, Germany) and mixed with 25 µL of the dye solution (1x HBSS + dye solution 1:250). Subsequently, plates were covered to be protected from light and incubated at 37°C for 60 min. The fluorescence of each well was measured in triplicate at 485 excitation/530 emission nm in a fluorometric plate reader. Three independent experiments with cells derived from three different donors were performed.

For the DMMB Assay, the same supernatant was used as in the CyQuant Assay. After adequate sample dilution, the DMMB solution (ApplyChem) was added (40 mM glycine

(Sigma-Aldrich), 40 mM NaCl (Carl Roth GmbH) at pH 3 and DMMB [8.9 mM in ETOH]). Chondroitin sulfate (Sigma-Aldrich) was used as standard. The absorption shift was measured at a wave length of λ = 633 nm to λ = 552 nm using a genios spectral photometer (Tecan Austria GmbH). Three independent experiments with cells derived from three different donors were performed.

2.11 RNA isolation

Scaffolds colonized with pACs and hMSCs were snap-frozen after 7, 14, 21, 28 and 35 days (each n = 3) and homogenized in RLT-buffer (Qiagen) with the Tissue Lyser for 2 times á 3 minutes at 50 Hz. RNA was isolated and purified using the RNeasy Mini kit according to the manufacturer´s instructions (Qiagen), including on-column DNAse treatment. Purity and quantity of the RNA samples were monitored (260/280 absorbance ratio) using the Nanodrop ND-1000 spectrophotometer (Peqlab, Biotechnologie GmbH, Erlangen, Germany).

2.12 Quantitative real time PCR

For cDNA synthesis 120 ng of total RNA was reverse transcribed using the QuantiTect Reverse Transcription Kit (Qiagen) according to the supplier manual. 20 ng cDNA was used for each quantitative real-time PCR (qRT-PCR) reaction using TaqMan Gene Expression Assays (Life Technologies) with primer pairs for type I collagen (Col1A1), type II collagen (Col2A1), aggrecan (ACAN), *SRY* (sex determining region Y*)-box 9* protein (SOX9) and the housekeeping gene β-actin (ACTB) as a reference gene **(Table 3)**. qRT-PCR was performed using the real time PCR detector StepOnePlus (Applied Bioscience (ABI), Foster City, USA) thermocycler with the program StepOnePlus software 2.3 (ABI). The relative expression of the gene of interests by the cells on the scaffolds was normalized to the ACTB expression and calculated for each sample using the ΔΔCT method as described by Schefe et al. 2006 [60].

Table 3 Sequences of primers used in the present study.

Gene symbol	Species	Gene name	Efficacy	Amplicon length (base pairs)	Assay ID *
ACAN	*Homo sapiens*	aggrecan	1.95	93	Hs00202971_m1
ACAN	*Sus scrofa*	aggrecan	1.69	60	Ss03374823_m1
ACTB	*Homo sapiens*	β-actin	1.89	171	Hs99999903_m1
ACTB	*Sus*	β-actin	1.71	77	Ss03376081_u1

	scrofa				
Col1A1	*Homo sapiens*	type I collagen	2.06	66	Hs00164004_m1
Col1A1	*Sus scrofa*	type I collagen	1.53	74	Ss03373340_m1
Col2A1	*Homo sapiens*	type II collagen	2.06 (1.9**)	124	Hs00264051_m1
SOX9	*Homo sapiens*	SOX9	1.92	102	Hs00165814_m1
SOX9	*Sus scrofa*	SOX9	1.57	145	Ss03392406_m1

*All primers from Applied Biosystems® (life technologies ™). **Primer efficacy determined for porcine chondrocytes

2.13 Immunocytochemical staining

The protein expression profile was assessed using CLSM. After the cultivation time cover slips (48 h, for MSC characterization) or scaffolds (14, 28 and 35 days) were fixed with 4% PFA (Morphisto GmbH, Frankfurt am Main, Germany) subsequently washed with TRIS buffered saline (TBS: 0.05 M TRIS, 0.15 M NaCl, pH 7.6) before incubated with protease-free donkey serum (5% diluted in TBS with 0.1% Triton X 100 for cell permeabilization) as a blocking step for 20 min at RT. Samples were incubated with primary antibody (see **Table 4**: CD29, CD34, CD44, CD45, CD90, CD105, vimentin, type II collagen, aggrecan, proteoglycans, SOX9) overnight at 4°C. Samples were rinsed with TBS before incubated with donkey-anti-rabbit-Alexa 488 (Invitrogen, Carlsbad, USA) or donkey-anti-mouse-cyanine-3 (Cy3, Invitrogen) coupled secondary antibodies (diluted 1:200 in TBS, see **Table 4**) for 1 h at RT. Cell nuclei were counterstained using 10 µg/mL 4′,6′-diamidino-2-phenylindol (DAPI, Roche, Mannheim, Germany). In addition, to the CD29 immunocytochemical staining of the hMSC colonized cover slips the F-actin was stained with Phalloidin Alexa488 (abcam, Cambridge, UK). Cover slips were rinsed with TBS and covered with Fluoromount G (Biozol Diagnostica Vertrieb GmbH, Eching, Germany) before examination by CLSM. Immunolabeled scaffolds were washed three times with TBS before examined by using CLSM. Three independent experiments were performed with representative microscopic fields. For the calculation of the “type II collagen area per cell”, three pictures of three independent experiments were taken and splitted with the ImageJ program in the “green” and “blue” channels. The green area was measured and related to the amount to blue dots (= cell nuclei).

Table 4 Antibodies used in the present study.

Target	Primary antibody	Dilution	Secondary antibody	Dilution
aggrecan	mouse anti human R&D systems, Minneapolis, USA	1:30	donkey-anti-mouse; Cy 3, Invitrogen	1:200
CD29	mouse anti human R&D systems, Minneapolis, USA	1:50	donkey-anti-mouse; Cy 3, Invitrogen	1:200
CD34	mouse anti human R&D systems, Minneapolis, USA	1:50	donkey-anti-mouse; Cy 3, Invitrogen	1:200
CD44	mouse anti human, CellSignaling Technologies, Danvers, USA	1:50	donkey-anti-mouse; Cy 3, Invitrogen	1:200
CD45	mouse anti human R&D systems, Minneapolis, USA	1:70	donkey-anti-mouse; Cy 3, Invitrogen	1:200
CD90	mouse anti human R&D systems, Minneapolis, USA	1:70	donkey-anti-mouse; Cy 3, Invitrogen	1:200
CD105	mouse anti human R&D systems, Minneapolis, USA	1:50	donkey-anti-mouse; Cy 3, Invitrogen	1:200
type II collagen	rabbit anti human, Acris Laboratories, Hiddenhausen, Germany	1:50	donkey-anti-rabbit, Alexa Fluor 488, Invitrogen	1:200
proteoglycans	mouse anti human, Chemicon International, California, USA	1:70	donkey-anti-mouse; Cy 3, Invitrogen	1:200
SOX9	rabbit anti human, Merck, Darmstadt, Germany	1:100	donkey-anti-rabbit, Alexa Fluor 488, Invitrogen	1:200
vimentin	mouse anti human, Sigma-Aldrich, Darmstadt, Germany	1:50	donkey-anti-mouse; Cy 3, Invitrogen	1:200

2.14 Statistics

The statistic description refers to all performed experiments. Data from all experiments are expressed as mean values with standard deviation (SD). Statistics were performed with GraphPad Prism8 (GraphPad software Inc., San Diego, USA). The normal distribution of the

results was analyzed using the Shapiro Wilk test. For comparison of groups a two-tailed one-way ANOVA (Fisher) was used followed by Tukey´s multiple comparison *post hoc* testing. The level significance (CI) was set at p values of ≤ 0.05 (*) and p values of ≤ 0.0001(****). Power of tests was 0.8. Three independent experiments with cells from three different donors were performed.

3. Results

3.1 Scaffold morphology and characterization

Not only pACs but also hMSCs were used to colonize a cubic BG scaffold with a pore size of 286.37±88.87 µm and a strut length of 112.98±12.13 µm. The struts had a diameter of 59.24±9.99 µm with a surrounding gel layer of 2 µm thickness **(Fig. 2)**.

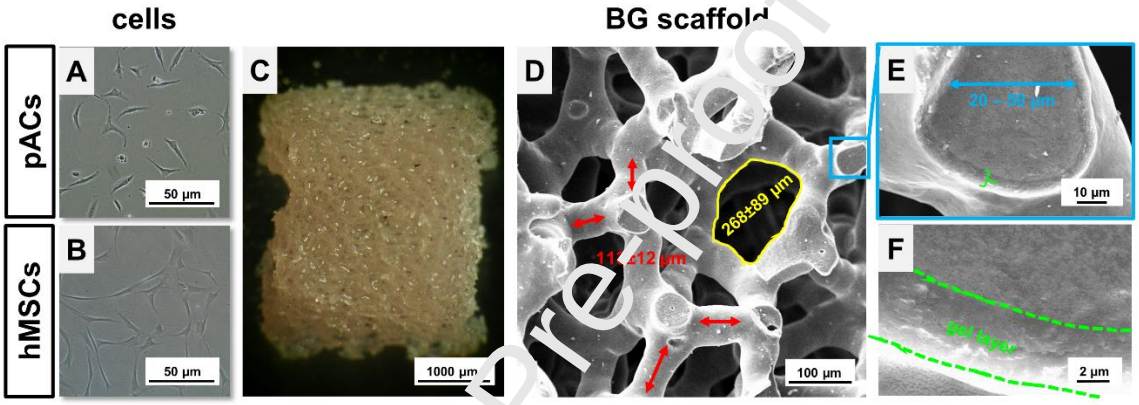

Figure 2 ***Primary cells used for future BG scaffolds colonization and scaffold topology.*** *Primary porcine articular chondrocytes (pACs)* ***(A)*** *and primary human mesenchymal stromal cells (hMSCs)* ***(B)*** *were seeded on a cubic BG scaffold* ***(C)****. Scanning electron micrographs displayed a detailed view of morphology, especially of the strut length (red arrows) and the pore size (yellow circle)* ***(D)****. At higher magnification the diameter of a strut (blue arrow)* ***(E)*** *and the gel layer* ***(F)*** *can be observed.*

3.2 Cytotoxicity, cell vitality and cytocompatibility of the scaffold

To assess whether the ion release of BG scaffold exerted cytotoxic effects on cells, cytotoxicity testing according to the national standard DIN EN ISO 10993-5 2009-10 norm was performed with the murine L929 fibroblasts as a testing cell line. Since pACs and hMSCs were used for the scaffold seeding experiments, these cells were also included in cytotoxicity testing. The normalized cell vitality was 102.69% ± 5.25 for L929, 98.14% ± 2.40 for pACs and 101.29% ± 6.81 for hMSCs. The positive control (treatment with 10% DMSO, data of all three cell species were pooled) was 11.42% ± 6.30 and the negative control (treatment with cell-specific growth medium) was 100% ± 3.87 **(Fig. 3A)**. The values of L929, pACs and hMSCs were normalized to the negative control and can therefore, be higher than 100%. Due to the fact that the growth medium was changed every second day only two-time points were chosen for pH measurement. The pH value of the growth medium without scaffolds was in a range of 8.1 ± 0.01, the pH value of the medium with uncolonized scaffolds was 7.8± 0.2 and the pH value of the medium with colonized scaffolds was 8.023 ± 0.1 (pACs) and 8.000 ± 0.24 (hMSCs). No significant differences were detected **(Fig. 3B)**.

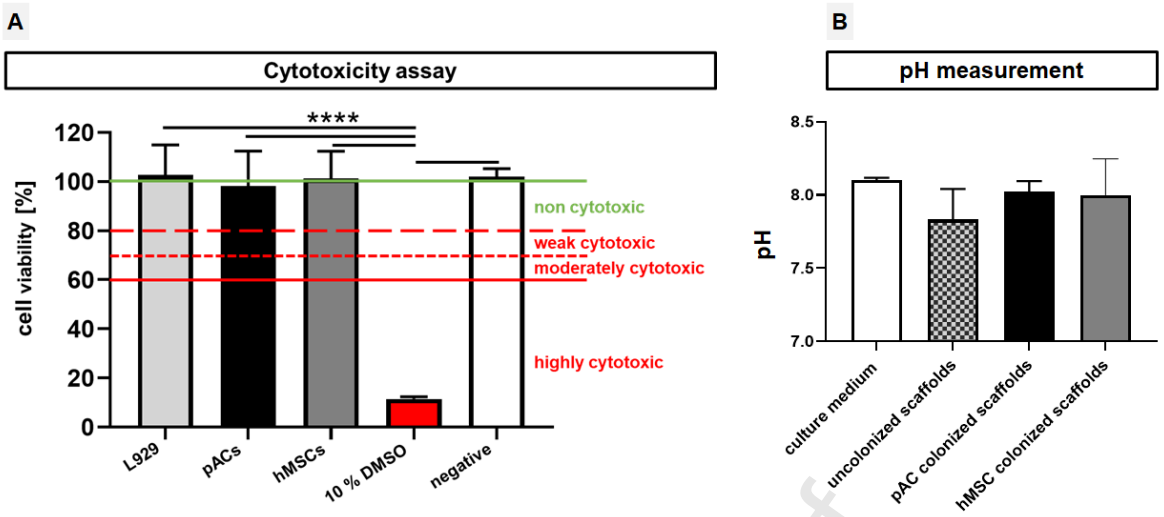

Figure 3 ***Cytotoxicity Assay of BG scaffold extracts (A) and pH measurement of growth medium exposed to the scaffolds (B)****. Viability of L929 (light grey), porcine articular chondrocytes (pACs, black) and human mesenchymal stromal cells (hMSCs, dark grey), treated for 24 h with BG scaffold extracts (48 h extraction) prepared from three different BG scaffold charges.* ***A:*** *Cell viability was above 70% in all cases. Positive and negative controls were performed with L929, pACs and hMSCs. Cell viability of the positive control with 10% dimethylsulfoxide (DMSO, red) was below 20% (highly cytotoxic) for all three cell species (data is pooled) and that of the negative control with culture medium (white) was set 100% for all three cell species. Cytotoxicity scale was taken from https://www.igb.fraunhofer.de/content/dam/igb/de/documents/broschueren/zte/Biologische_Beurteilung_von_Medizinprodukten_Pruefungen_auf_in_vitro_zytotoxizitaet_nach_din_iso_10993_5.pdf (downloaded: 05.08.2020). The CellTiter 96®Aqueos One Solution Cell Proliferation Assay was used to assess cytotoxicity. n=3. Ordinary one-way ANOVA with multiple comparison, p values: **** < 0.0001.* ***B:*** *The pH (at RT) of the fresh growth medium without scaffolds (white), the pH of uncolonized scaffolds (checkered), the pH of pAC-colonized scaffolds (black) and the pH of hMSC-colonized scaffolds (grey) was measured. No significant differences were detected using unpaired t-test (n=3).*

The vitality assay proved survival of pACs and hMSCs up to 5 weeks of culture on the scaffolds. Viable cells were labeled by FDA, a green fluorescence marker with cytoplasmatic distribution, whereas dead cells were labeled by PI, a red fluorescence marker intercalating into DNA when the nuclear membranes become permeable thereby showing nuclear distribution. The majority of the chondrocytes attaching to the struts was vital during the five weeks of observation time and spread over the whole scaffold surface around the pores **(Fig. 4A-E)**. Spread chondrocytes could be detected, which nearly completely colonized the scaffold surface. No difference in viability of pACs could be observed during the entire cultivation time. In contrast to the pACs, the hMSCs formed cell clusters around the struts and inside the pores after 7 days after colonization. After 14 days the hMSCs tried to spread around the struts and their cell shape was getting more and more elongated. After 21 days hMSCs lost their contact to the scaffold, leading to a decreasing amount of cells on the scaffold. After 35 days only some single cell clusters could be detected **(Fig. 4F-J).** The evaluation of the migration depth of the cells into inner parts of the scaffold was impossible because the BG scaffolds could not be transected due to being too brittle.

Nevertheless, the calculated percentage of colonized scaffold surface covered by vital pACs was slightly increasing and reached nearly 100% after 35 days (**Fig. 4KA**), which indicated

that only vital cells could be found on the struts. The total scaffold surface percentage covered with vital cells decreased (27%) after 14 days in the pAC scaffold cultures and then increased again up to 49% surface area until day 35 (**Fig. 4L,** not significant). The cell vitality of hMSCs increased significantly after 21 days compared to 7 and 14 days **(Fig. 4M)**. In the hMSC culture, a smaller surface area (21%) was colonized with vital cells after 7 days in comparison to the pACs and a continuous decrease of the surface area displaying living cells could be calculated reaching less than 10% after 35 days **(Fig. 4N,** no significant differences**)**.

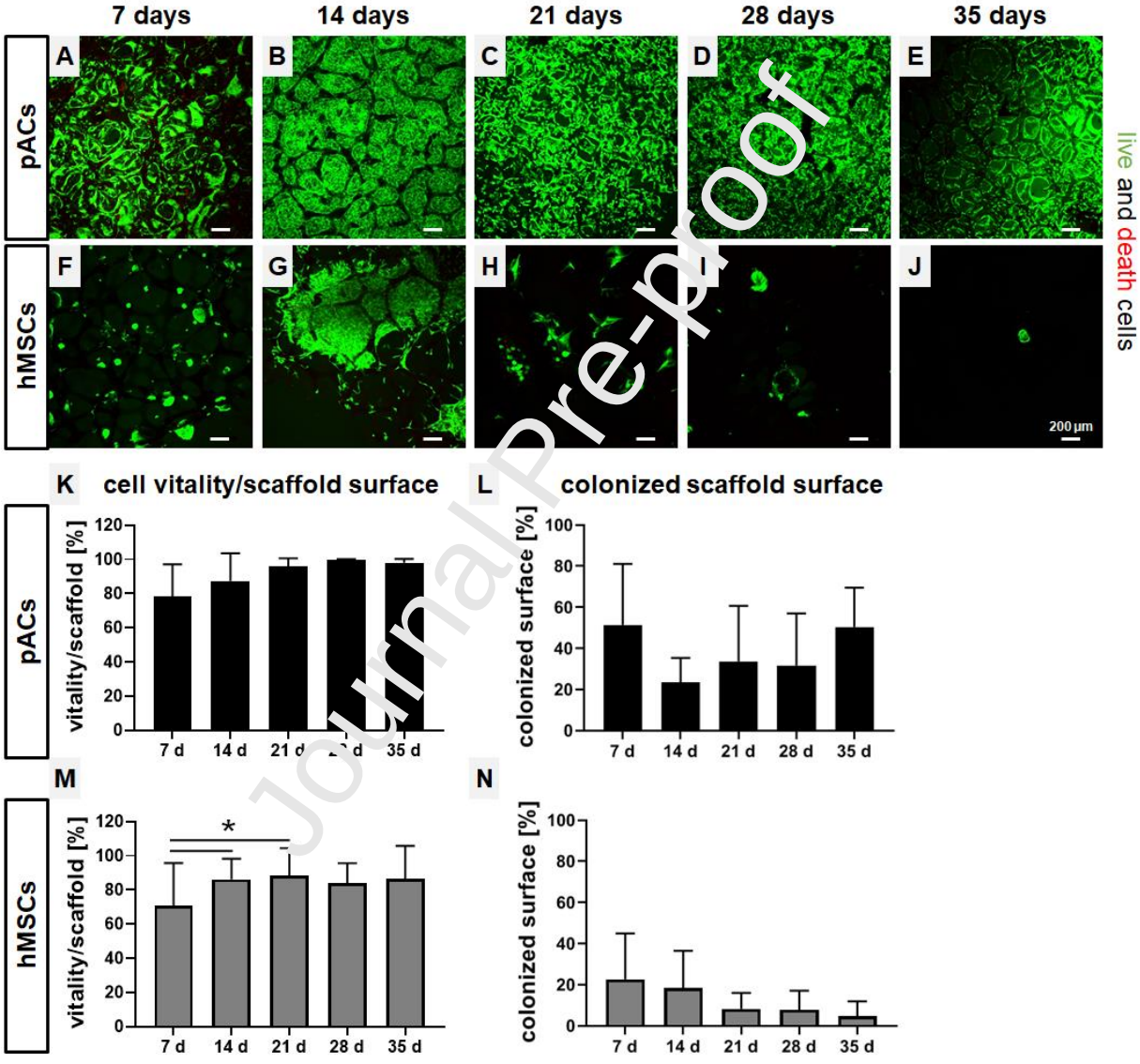

Figure 4 ***Vitality Assay of colonized BG scaffold and calculation of cell vitality per scaffold surface and colonized scaffold surface.*** *Representative pictures of three independent experiments show vital (green) and dead (red) porcine articular chondrocytes (pACs)* ***(A – E)*** *and human mesenchymal stromal cells (hMSCs)* ***(F- J)*** *over a cultivation time of 7 to 35 days. pACs vitality per scaffold surface* ***(K)*** *and the colonized scaffold surface* ***(L)*** *over the whole cultivation period. Results of hMSCs vitality per scaffold surface* ***(M)*** *and the colonized scaffold surface* ***(N)*** *over the whole cultivation period. Three independent experiments (n=3) with cells from three different donors were performed. One-way ANOVA combined with post hoc Tukey´s multiple comparison between groups: p values: * <0.05. Scale bar: 200 µm*

3.3 Ultrastructure of pACs and hMSCs on bioactive glass scaffold

Analysis of the pore sizes and the cell attachment of pACs and hMSCs was performed with SEM. After 14 days, the struts and pore walls were nearly completely colonized with cells. The cell shape of pACs was rounder in comparison to the hMSCs, which had longer spindle-shaped cell bodies with a high number of filopodia. Both cell types started to synthesize a fibrous ECM that covered the scaffold surface. After 28 days the struts and pores were filled with pACs which formed a homogenous layer covering the struts. hMSCs were found only in selected areas, whereas the pACs were homogenously distributed. Both cell types maintained their typical cell shape **(Fig. 5)**.

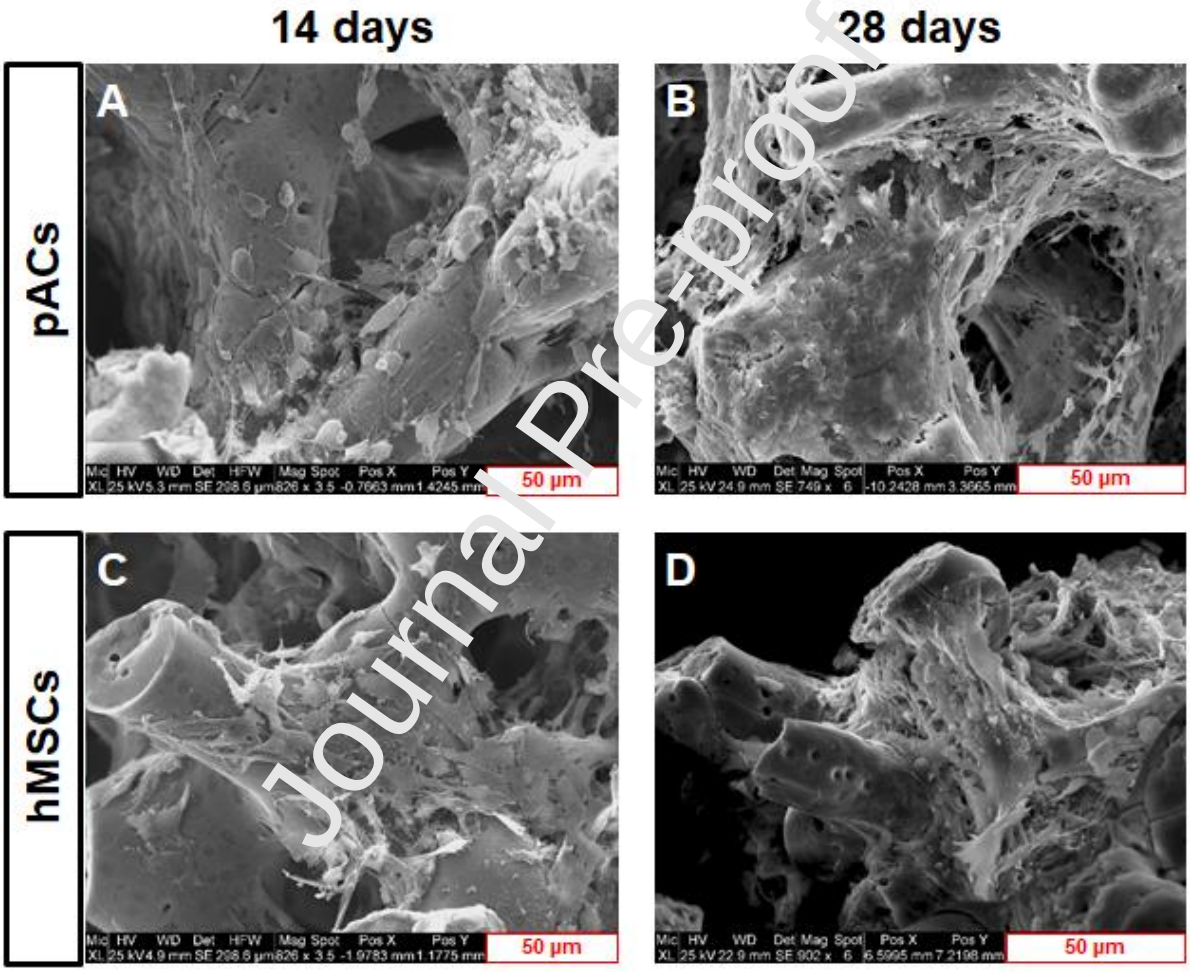

Figure 5 ***Scanning electron microscopy (SEM) of colonized BG scaffolds.*** *Cell morphology of the pACs* ***(A, B)*** *and hMSCs* ***(C, D)*** *on the BG scaffold after 14 days* ***(A, C)*** *and 28 days* ***(B, D)*** *in culture. Differences in cell shape and distribution on the struts can be seen. Scale bars of 50 µm.*

3.4 Cell type and time dependent proliferation and sGAG synthesis

The cell number per scaffold was determined at different time points by measurement of DNA content and using a cell number standard curve to calculate the DNA content per cell in

order to estimate the final cell proliferation. During the 21 day cultivation period on the scaffold, the DNA amount of pACs was significantly decreased (from 370.000 to 60.000) and significantly increased until 35 days after seeding (260.000). In general, the cell number of hMSCs in the scaffold was reduced in comparison to the pACs. After a slight increase until day 21 (150.000 cells per scaffold), the cell number was decreasing until day 35 (30.000) **(Fig. 6A, C)**.

The sGAG content per pAC cell increased from 7 days and reached the highest level after 21 days (1.1 ng), followed by a decreasing trend. In contrast to the pACs, the hMSCs showed a decreasing trend with the lowest level after 21 days (0.35 ng/cell). But the sGAG content increased and reached the highest amount after 35 days (1.55 ng/cell) **(Fig. 6B, D)**.

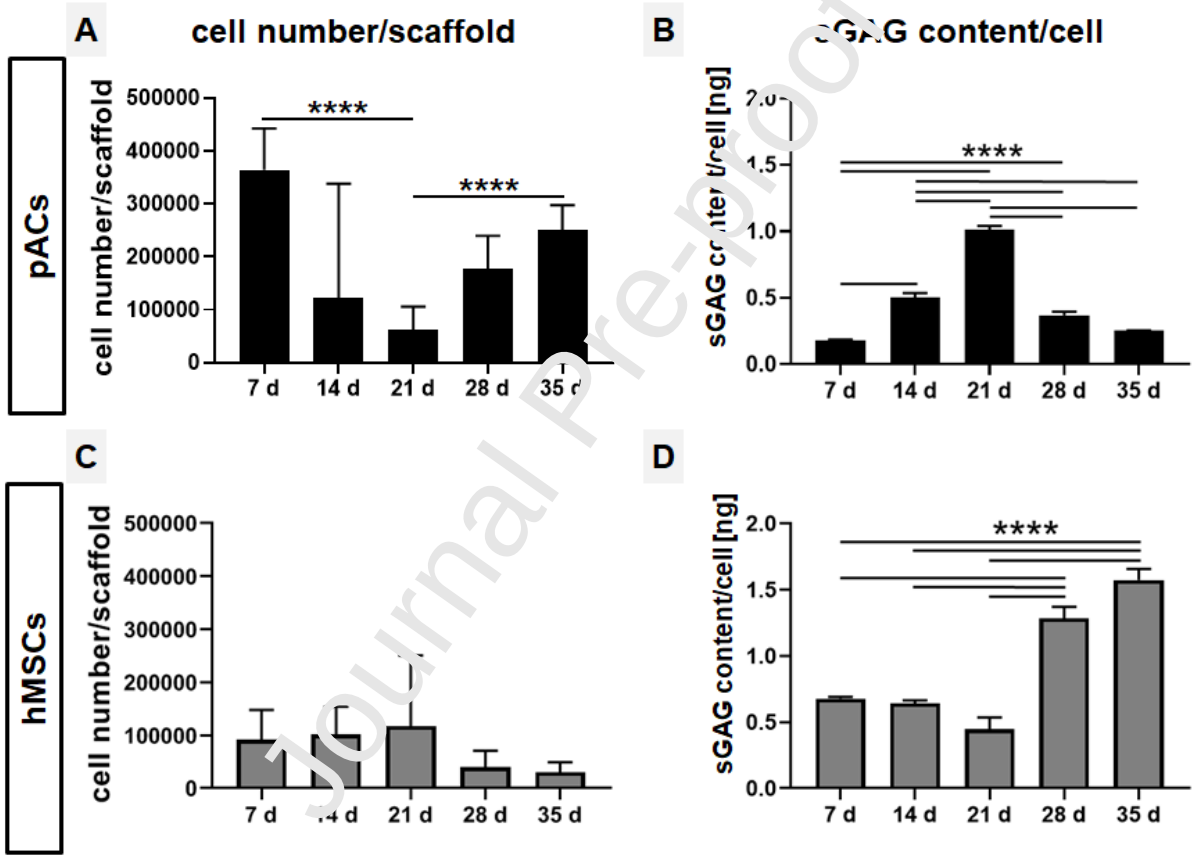

Figure 6 ***Calculation of cell numbers per scaffold and sulphated glycosaminoglycan (sGAG) content per cell.*** *Results of the cell number* ***(A)*** *and the sGAG content* ***(B)*** *of BG scaffolds colonized with pACs over the whole cultivation period. Results of the cell number* ***(C)*** *and the sGAG content* ***(D)*** *of BG scaffolds colonized with hMSCs over the whole cultivation period. Three independent (n=3) experiments with cells of three different donors were performed. One-way ANOVA (post-hoc Tukey Test) for comparison between the groups. p values: * <0.05; **** <0.0001. pACs, porcine articular chondrocytes; hMSCs, human mesenchymal stromal cells.*

3.5 Articular chondrocytes show gene expression of cartilage-specific marker type II collagen and aggrecan

Real-time PCR analysis was carried out for several cartilage-associated genes to estimate the effect of BG on pACs and hMSCs after 7, 14, 21, 28 and 35 days of cultivation in a 3D

cubic scaffold. Gene expression of type II collagen, as the most important cartilage marker, and aggrecan as well as type I collagen and SOX9 was detected in pACs. Type I and II collagens, aggrecan and SOX9 were assessed in hMSC cultures. The results showed that the relative gene expression of type I and II collagen, aggrecan and SOX9 decreased with increasing cultivation time in BG scaffolds colonized with pACs. The relative gene expression of type I and II collagen was the highest after 14 days and after 7 days that of aggrecan and SOX9. The hMSCs cultures showed an upregulation of the relative gene expression of type II collagen, while the relative gene expression of aggrecan was the highest in comparison to the other four time points analyzed. hMSCs had no relative gene expression of type II collagen after 28 and 35 days. Although the relative gene expression of type I collagen increased within the first two weeks of cultivation, it decreased and had the lowest level after 35 days. The relative gene expression of SOX9 also decreased after 21 days **(Fig. 7)**.

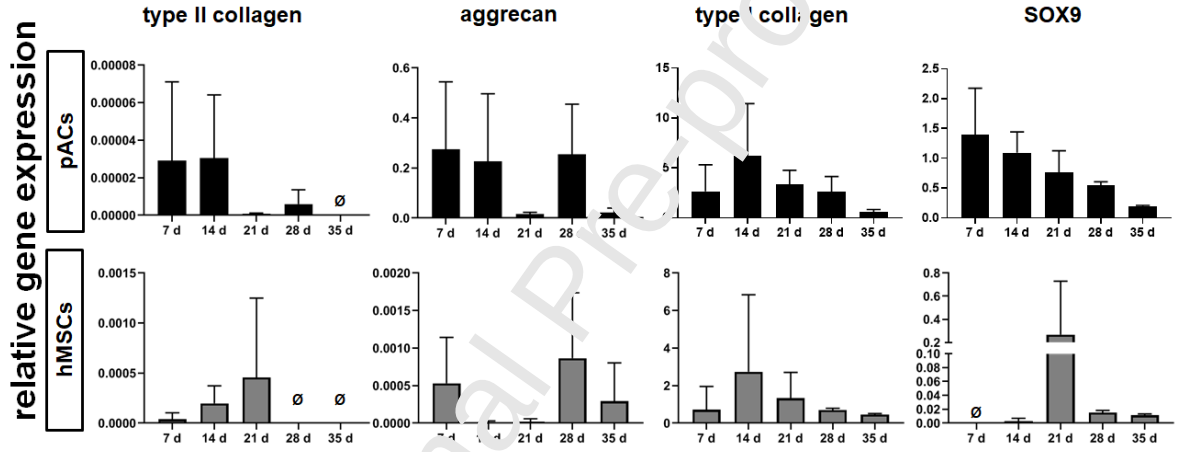

Figure 7 ***Gene expression level for cartilage extracellular matrix components and the transcription factor SOX9 after 7, 14, 21, 28 and 35 days in the BG scaffold.*** *Relative gene expression of type II collagen, aggrecan, type I collagen and SOX9. All diagrams summarize n=3 independent experiments with cells of three different donors and show means with standard deviation. No significant differences could be calculated after One-way ANOVA (post-hoc Tukey Test). Gene expression was normalized to the reference gene β-actin (ACTB). pACs, porcine articular chondrocytes; hMSCs, human mesenchymal stromal cells.*

3.6 Characterization of undifferentiated human mesenchymal stromal cells

Typical surface marker expression such as CD29, CD90, CD105 and also vimentin could be depicted in the undifferentiated hMSCs and markers were localized using immunocytochemical staining. The CD34 and CD45 expression on the hMSCs was not detectable **(suppl. Fig. 1)**.

3.7 Cartilage-specific ECM protein expression

For evaluation of cartilage-specific ECM protein expression immunocytochemical analysis was carried out. The pACs and hMSCs were cultured for 14 and 28 days before being immunolabeled for type II collagen (green) and cartilage-specific proteoglycans (red). Type II

collagen was present around and between the cells in their freshly produced ECM. In scaffolds colonized with pACs, type II collagen was more prominent and more evenly distributed around the cells, in contrast to the hMSCs, where it was associated with the cell clusters after 28 days. At day 14 days the type II collagen immunoreactive area was significantly larger around hMSCs in comparison to that in the pAC cultures. However, after 14 days the area increased around pACs and significantly decreased around hMSCs **(Fig. 8)**. The calculation of the collagen immunoreactive area per cell showed that hMSCs produced significantly more type II collagen after 14 days than pACs. After 14 days of further cultivation the pACs continuously expressed type II collagen, while the area per cell positive for type II collagen decreased to 0.05% in hMSCs scaffold cultures **(Fig. 8E)**.

The cartilage-specific proteoglycans **(Fig. 8F-J**, red**)** and the transcription factor SOX9 **(Fig. 8K-O,** green**)** were also evaluated after 14 and 28 days of culturing both cell types on the scaffold using immunocytochemical staining. Cartilage-specific proteoglycans could be observed in the 14 and in the 28 days-old pACs cultures **(Fig. 8F and G)**. The cartilage-specific proteoglycan expression tended to increase during the cultivation time in the scaffold cultures with pACs (**Fig. 8J**). In comparison to pACs the hMSCs expressed a significantly lower amount of cartilage-specific proteoglycans on the bioglass (**Fig. 8F-J**). During the cultivation time a downregulation of the cartilage-specific proteoglycan expression (not significant) could be observed in hMSC scaffold cultures (**Fig. 8J**). SOX9 expression of pACs was observed after 14 days and after 28 days (**Fig. 8K and L**). It increased during the cultivation period in pACs cultivated on the scaffolds (**Fig. 8O,** not significant). In contrast to the pACs, the immunoreactivity of SOX9 was weaker in hMSCs and decreased after 28 compared to 14 days (**Fig. 8O**, not significant).

A type II collagen (green) and cartilage-specific proteoglycan (red) expression of pACs could be proven after 35 days. In the detailed view type II collagen expression appeared around the cells and was more intensive than the cartilage-specific proteoglycan expression (**suppl. Fig. 2A, B**). The negative control proved that the antibodies bound specifically and exerted no unspecific binding to the BG. Additionally, no autofluorescence of the BG could be observed **(suppl. Fig. 2C, D)**.

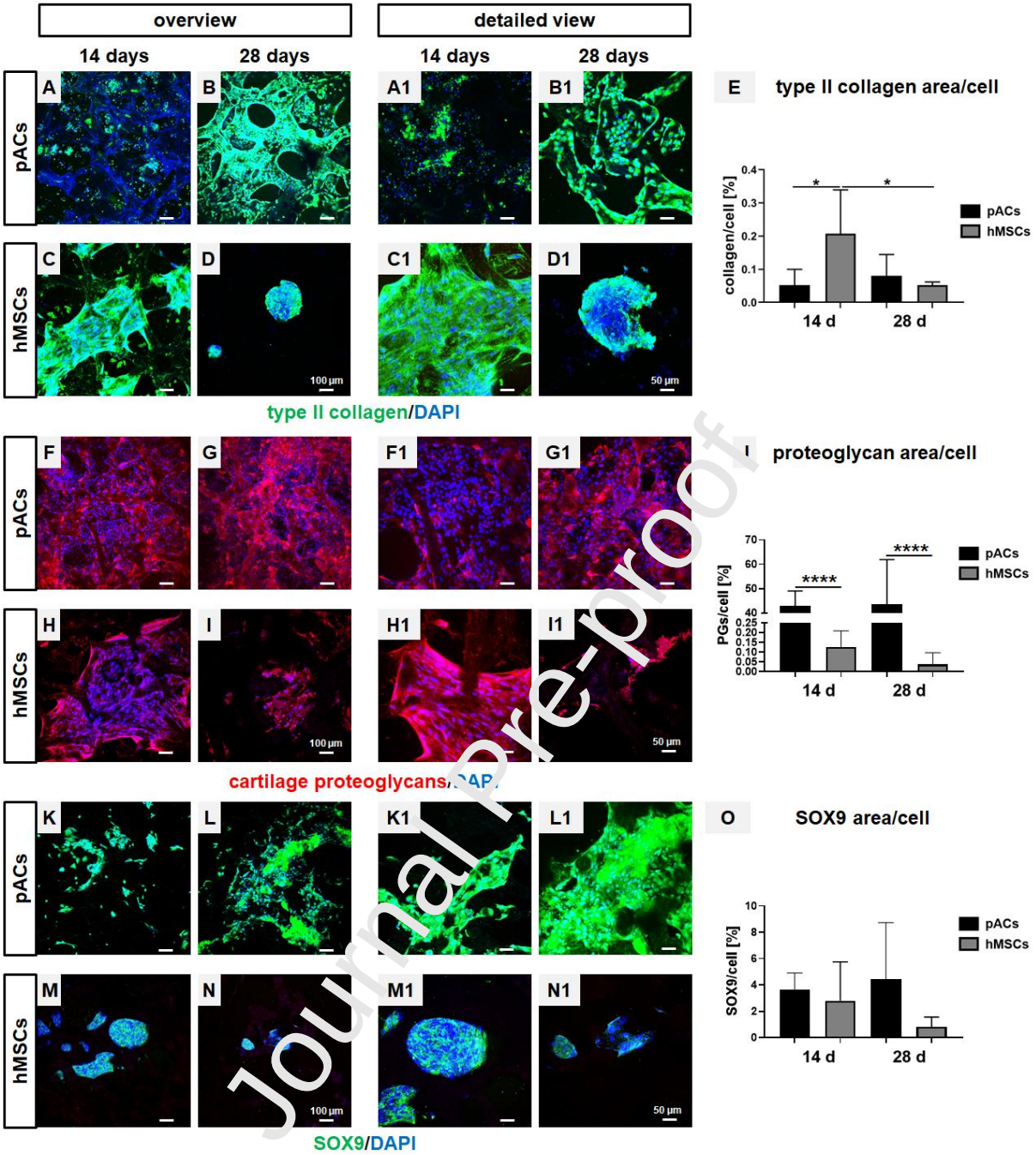

Figure 8 ***Protein expression of type II collagen, cartilage-specific proteoglycans and SOX9.*** *Representative immunocytochemical staining of type II collagen (green) and cell nuclei (blue) of pACs* ***(A, B, A1, B1)*** *and hMSCs* ***(C, D, C1, D1)****. Calculation of the type II collagen area per cell* ***(E)****. Immunocytochemical staining of proteoglycans (red) and cell nuclei (blue) of pACs* ***(F, G, F1, G1)*** *and hMSCs* ***(H, I, H1, I1)*** *with the evaluation of the proteoglycan (PG) area per cell* ***(J).*** *Immunocytochemical staining of SOX9 (green) and cell nuclei (blue) of pACs* ***(K, L, K1, L1)*** *and hMSCs* ***(M, N, M1, N1)*** *with the evaluation of the SOX9 area per cell* ***(O).*** *An overview* ***(A, B, C, D, F, G, H, I, K, L, M, N)*** *and at higher magnification* ***(A1, B1, C1, D1, F1, G1, H1, I1, K1, L1, M1, N1)*** *after 14* ***(A, A1, C, C1, F, F1, H, H1, K, K1, M, M1)*** *and 28 days* ***(B, B1, D, D1, G, G1, I, I1, L, L1, N, N1)*** *scaffold cultures. n=3. One-way ANOVA (post-hoc Tukey Test) for comparison between the groups. p values: * <0.05; **** <0.0001. pACs, porcine articular chondrocytes; hMSCs, human mesenchymal stromal cells*

4. Discussion

The self-regeneration capacity of the adult articular cartilage is strongly limited due to its avascularity, low cellularity and the fact that it is a bradytrophic tissue [57]. Clinical requirements show the need to develop new strategies for cartilage repair [61]. To date,

there is no cost-effective cartilage regeneration that is providing long-term OA prevention after cartilage defects. Both therapeutical approaches (ACI and MACI) are cost-intensive as well as surgeon- and lesion-dependent [62-64]. Success of a potential cartilage implant is based on an intimate cell/material interaction, which allows chondrogenesis [65]. For cartilage tissue engineering, as a promising approach to develop novel strategies for cartilage repair, the scaffolds should have a high biocompatibility, provide a large surface for sufficient cell attachment and proliferation as well as have an adequately adapted degradation rate to be substituted by the newly formed tissue [20]. Chondrocytes should not lose their chondrogenic phenotype and maintain their ECM production in a 3D environment [66-68]. Hence, we designed a highly porous bioactive scaffold with interconnecting pores which should be replaced by cartilage ECM prospectively [20]. Nevertheless, the high porosity, interconnectivity and a regular strut structure could be visualized by the SEM and allowed not only the pACs but also the hMSCs to migrate and homogeneously distribute on the BG scaffold surface. A suitable raw glass composition was selected to achieve BG scaffolds which withstand longterm culturing. Basically, the novel BG developed in the present study consists of SiO_2, P_2O_5, B_2O_3, and Na_2O+K_2O and a leaching process leads to the formation of a silica gel layer on the struts. However, this layer can also change the thickness of the struts and thus, influence the porosity of the scaffold. Strut length (around 113 µm) and pore sizes (around 285 µm) were selected to allow a chondrogenic differentiation in agreement with a previous study [69], since chondrogenic cell types pACs and hMSCs were chosen for scaffold colonization. Due to the fact that the amount of healthy autologous cartilage available for harvesting is very limited and taking a biopsy in the joint is an invasive procedure, hMSCs were included in the experiments which can be more easily harvested. Undifferentiated hMSCs represent an alternative chondrogenic cell type suitable to evaluate their chondrogenic response when exposed to the BG scaffold mediated by its particular bioactivity and topology including distinct 3D surface structure, porosity and pore size [70]. The structural design of scaffolds, like porosity, pore size and interconnectivity as well as surface structure facilitates cartilage regeneration [71]. The size of the pores is decisive for the differentiation and maintenance of the typical cell phenotype, especially of chondrocytes and hMSCs [72]. Because of the cell size variation of chondrocytes (12 – 40 µm) [73, 74] and of MSCs (12 – 30 µm) depending on culture conditions [75], the pore size was chosen within a range of around 285 µm to allow also to harbor cell aggregates. A comparable pore size (200 µm) was also suitable for chondrogenic differentiation of primary and immortalized hMSCs in previous studies [69, 76]. Other research groups reported migration and deposition of a mineralized ECM by BMSCs in even large-pored scaffolds (450 – 600 µm) [72]. However, it might not be ideal to harbor the self-aggregated MSCs clusters of different sizes observed in the present study during longterm culturing. hMSC clusters were

only loosely attached to the scaffold struts and might be lost due to fluid flow under the dynamic culturing conditions applied.

The ideal scaffold topology (e.g. pore size, surface roughness) required for chondrocyte and undifferentiated hMSC adhesion differs and might not be selected for the hMSCs at the current state. It has to be adapted in future. MSCs prefer larger pores than chondrocytes [69] but the pores used here might be too large (around 285 µm) to capture the smaller cell aggregates. In addition to pores, surface topology presents an important issue for cell differentiation. Enhanced proliferation of hMSCs by activating the extracellular regulated kinase (ERK) pathway through silicon ions was also depended on the size of BG particles included into a composite material [77]. Our scaffold consisting of 100% BG presented so far a rather smooth surface except for some drop-like pits as shown by SEM. The influence of different degrees of surface roughness on chondrogenesis could be addressed in future as well as the effect of BG particles on chondrocytes and MSCs. Nevertheless, we believe that the composition is crucial and could be further changed in future to enhance initially proliferative activity, to maintain adherence of MSCs and further stimulate their expression of chondrogenic genes.

The question why hMSCs do not maintain their longterm adherence on Car12N forming compact clusters can probably not be answered by the scaffold topology but rather by its composition. The pure BG scaffold characterized in the present study was mainly based on silicon (SiO_2) and phosphate (P_2O_5) ions and of many other ions (B_2O_3, Na_2O and K_2O). The ion composition is very important, not only for the ion release in response to leaching and the subsequent degradation process, but particularly for the cell behavior. In recent years, many authors tried to find out how the dissolved ions influence the cells. SiO_4^{4-} ions for example enhanced the proliferation and differentiation of osteoblasts through activating the *Wingless* and *integration site-1* (Wnt1)/β-catenin and Mitogen Activated Protein kinase signaling pathways [78]. Additionally, an increased proliferation of osteoblasts could be shown in 45S5 BGs plus titanium and boron ions, but in contrast, iron- and fluorine-containing glasses reduced their proliferation [79]. Hence, Car12N contains titanium and boron but no iron (**Table 2)**. The effect of BG45S5 and BG60S, the latter contains 60% silicon but lesser CaO than BG45S5, was also tested on fetal nasoseptal chondrocytes which modulated their differentiation program in an osteogenic direction especially in response to BG45S5 [80]. Since the osteogenic lineage differentiation is unwanted, Car12N contains higher amounts of silicon but no CaO (**Table 1**).

Beryllium is an alkaline earth metal, which specifically inhibits regeneration *in vitro* and *in vivo* though disruption of cell migration and cell cycle progression, especially the G2/M phase [81]. Due to the fact that Be^{2+} leads to an increase in senescence regulators (p53 and p21) in human fibroblasts [82], we have not added this ion to our glass composition. Mg^{2+} ions play

an essential role in cell attachment through the binding interaction between the integrin family of cell surface receptors and their ligand proteins [83]. This effect could be also shown in hMSCs, additionally leading to a higher proliferation rate and an accelerated osteoblastic differentiation [84]. In combination with silicon and released phosphate ions, Ca^{2+} contributes to the formation of hydroxyapatite and is therefore, interesting for bone tissue engineering [85]. Mg^{2+} might also contribute to hydroxyapatite formation [86]. Altogether, not only Mg^{2+}, but also Ca^{2+} and Sr^{2+} are osteoinductive, promote the osseo integration of calcium phosphate-based scaffolds and stimulate osteoblasts [87, 88]. Barium (Ba), another alkaline earth metal, acts in low doses as a muscle stimulator [89]. To avoid osteogenic differentiation of chondrocytes and unwanted effects, all these alkaline earth metal ions were not included in Car12N. Car12N might contain only few ions needed for function of cell-ECM and cell-cell adhesion receptors on MSCs. This hypothesis could explain the phenomenon of hMSC cluster formation with increasing cultivation time. Integrins, particularly the β1 chain [90] and cadherins (e.g. N cadherine in MSCs [91, 92] operate as cell-ECM and cell-cell contact molecules and require divalent cations for their function. Hence, the absence of these alkaline earth metal ions in the novel BG might be partly responsible for the lack of cell adhesion of the MSCs on the material. In this case the pACs are less sensitive to impaired divalent Mg^{2+} and Ca^{2+} supply. In chondrocytes, the concentration of calcium plays also a decisive role not only in maintaining the phenotype and activating chondrocyte-specific transcription factors but also in cell-ECM interaction [93]. The culture media for both cell types contained $CaCl_2$ and $MgSO_4$. More of the Ca^{2+} and Mg^{2+} were in the MSC compared to the chondrocyte growth medium. Concerning the additional supplements for the growth media 10% FCS was used for chondrocytes and 5% PL for hMSCs which could also influence cell performance in regard to adherence. However, the hMSCs might need more ions than available due to the fact that these cells are more active during chondrogenic differentiation and internalize Ca^{2+} ions for cadherin function. Intracellular Ca^{2+} storage capacity might differ between both cell species. One could also hypothesize that some ions released from the bioglas might capture essential divalent ions from the MSC growth medium which are essential for MSC adhesion. In contrast to mature chondrocytes, chondrogenically differentiating MSCs undergo intensive cell-cell interactions (forming cell aggregates mimicking the so-called mesenchymal condensation phase during embryogenesis) before starting later more intensive cell-ECM interactions [91] and hence, adherence to the substrate. For these cell-cell interactions Ca^{2+}-dependent N-cadherin plays a pivotal role [92, 94]. Obviously, the Car12N scaffolds supported MSCs self-aggregation in the scaffolds suggesting the onset of their differentiation.

Changes of cell shape can be explained by the intracellular Ca^{2+} content, which was not measured in our study [95]. Nevertheless, the formation of hMSC clusters and a decreasing

DNA amount after 42 days irrespectively of maintained vitality could also be observed by another research group on a collagen matrix supplemented with BG45S5 particles [96].

In contrast to many other experiments where BGs were used as a secondary component for stabilizing the main construct (consisting polymers, ceramics and hydrogels) and as an ion releaser during the leaching process [97-99] we developed a scaffold consisting of 100% of BG Car12N. The high cytocompatibility of the scaffolds was proven by the vitality assay of pACs and hMSCs on BG scaffolds, especially the surface colonized after 35 days with pACs was remarkable, with an almost negligible amount of dead cells. A defined cytotoxicity test according to the national standard DIN EN ISO 10993-5 2009-10 norm was performed. With its help it could be excluded that a profound ion release within 48 h might lead to cell intolerance. Cytocompatibility could also be supported by the pH measurement because there were no significant differences between before and after the scaffold colonization. For other BG species a clear shift of the pH in the alkaline direction is known. BG45S5 particles led to an increase in intracellular Ca^{2+} of osteoblasts and an internal and external ion balance into the alkaline direction [100]. It has to be mentioned that the pH measurement took place at RT and not under culture conditions (37°C, 5% CO_2), which could very slightly influence the pH.

Vitality assay, immunocytochemical staining and SEM pictures showed that both cell types colonized the scaffold surface evenly after 14 days. The exact cell count could not be calculated from the images due to confluent cell growth on the scaffolds; therefore, the cell number per scaffold during culturing were determined based on the DNA content. The cell amount of pACs decreased significantly at day 21 of culture before recovering again by cell proliferation to a significantly higher level compared to day 21. It presented at the end of culture no significant difference to the pAC numbers calculated at the beginning of the culture. This biphasic trend of DNA content could also be seen in another study with bovine articular chondrocytes cultured on biodegradable polyurethrane scaffolds [101].

It has been reported that dynamic stimulation amplifies cellular DNA synthesis [102]. For this reason, a dynamic culture system was selected in the present study. However, the decrease in numbers of hMSCs after 28 days (not significant) was not fully understood because the scaffolds were kept for the whole observation period under a slight shear stress by dynamical culturing. Other authors reported an increase in the DNA content during long-time cultivation of scaffolds colonized with MSCs and functionalized with BG (45S5 and mesoporous BG) particles [103, 104]. It is possible that the dynamic rotation culture used in the present study did not provide a sufficient chondrogenic stimulus for the cells, as it is known that not only chondrocytes but also BMSCs cultured on scaffolds increase their GAG synthesis during mechanical compression [105]. The presence and amount of ECM components such as the total collagen content but also the homogenous scaffold structure led to an improvement of

its mechanical strength [106]. The sGAG content per cell was highest at day 21 in pAC scaffold cultures and increased in the scaffolds colonized with hMSCs at the end of the culture.

Interestingly, there was an opposite trend in the cell numbers and the sGAG content in pACs at the same observation time points. In the beginning of scaffold culture, a matrix formation phase can be hypothesized in pACs, in which sGAGs are synthesized, but the pACs do not proliferate. Then, a phase of increased proliferation follows, in which the cells reduce their sGAG synthesis. Accordingly, the DNA content of pACs slowly decreased and the amount of sGAGs increased at the same time and later *vice versa*. In hMSCs a comparable trend was visible, but occurred delayed, starting with proliferation on the scaffolds accompanied by low sGAG production. This might reflect their undifferentiated phenotype in the beginning and suggests later (between 21th and 28th days of scaffold culture) the onset of chondrogenic differentiation characterized by an increased amount of sGAGs and higher Sox9 and aggrecan gene activity. This might reflect the conditions of chondrocytes in the growth plate [107]. In both cell types the 21th day seems to represent a turning point.

In addition to the sGAGs, cartilage-specific collagens (e.g. type II, type IX, type XI collagen) and hyaluronan are also found in the cartilage ECM, which is built up by relatively few chondrocytes [1, 108]. The relative gene expression of type II collagen, as the most prominent collagen type in cartilage [1], was downregulated in the pAC cultures. Bovine articular chondrocytes seeded on a polyurethane scaffold also showed a continuous reduction of relative gene expression of type II collagen during the longtime culture of 42 days [101]. Nevertheless, the specific synthetic activity and the maintenance of the chondrogenic phenotype could still be concluded based on the protein expression of type II collagen detectable after 28 days in both pAC and hMSC scaffold cultures. In contrast to other studies, chondrogenic differentiation of undifferentiated hMSCs occurred here without any supplementation with chondro-inductive mediators, growth factors, such as transforming growth factor beta 1 (TGF-β1) or application of hypoxia [109-111] suggesting bioactivity of the Car12N BG scaffolds.

Aggrecan is the major proteoglycan in articular cartilage and protects the tissue under load [112]. The degradation of aggrecan in the native tissue is documented as a typical feature of cartilage degeneration in OA patients [113]. In general, the relatively higher expression of aggrecan in comparison to type II collagen could also be observed by other authors in chondrocyte 3D cultures [114]. The relatively high gene expression of aggrecan at 28 days in cultures of both chondrogenic cell types and the upregulation of the relative gene expression of transcription factor SOX9 in the hMSC culture at 21 days suggests an ongoing chondrogenic maturation process [115]. SOX9 also regulated the transcription of type II collagen, which increased the synthesis of cartilage-specific ECM, especially at day 21 in the

hMSC culture [115]. SOX9 protein could also be detected in scaffold cultures of both cell types at both investigation time points, but to a higher extend in the pAC cultures, suggesting a higher degree of chondrogenic differentiation compared with the hMSCs. This assumption is supported by the more pronounced immunoreactivity of collagen type II and adult cartilage proteoglycans in hACs compared to hMSCs.

The handling of our newly developed scaffolds after 35 days of cultivation indicates that it was still stable and the degradation process has not yet proceeded. Cartilage repair requires time and hence, slowly degrading biomaterials. Detailed analysis of the amount of ion release, gel layer thickness and reduction of strut thickness after longtime cultivation conditions are addressed by currently ongoing work. The evaluation of the migration depth and therefore, the colonization of the inner parts of the scaffold was not possible because of the brittleness. Also, paraffin embedding and following histological staining (hematoxylin eosin or alcian blue) to evaluate the overall cell distribution and their surrounding proteoglycans inside the scaffold could not be performed and therefore, were not compared to other studies [69, 116]. In further investigations, the scaffold should be colonized with differentiated hMSCs under mechanical stimulations for enhancement of neocartilage formation mimicking chondrogenesis [117]. Additionally, more cartilage related proteins, like cartilage oligomeric protein (COMP), versican and matrilin-3, should be analyzed to prove the stabilization and the maintenance of the ECM and its biochemical properties [108, 118, 119]. Another limitation of this study, which should be addressed in future, is the measurement of the pH value in the cell culture for further time points because the fibril formation of type II collagen, the number of gap junctions and the activity of the adenylate cyclase that regulates many pH dependent metabolic pathways depend on pH [120-122].

5. Conclusion

In this study a completely novel bioactive glass composition (Car12N) was created, which contains no alkaline earth metal ions preventing hydroxyapatite deposition unwanted in cartilage and causing no alkaline pH shift. The BG could be used to prepare scaffolds consisting of 100% Car12N with a high cytocompatibility, with a topology tailored for cartilage tissue engineering. The present results confirmed that the pure BG scaffolds allow the adherence, proliferation and sGAG synthesis of pACs and hMSCs. The sustained protein expression of type II collagen and cartilage-specific proteoglycans of pACs after 28 days of culturing indicates the maintenance of their chondrogenic phenotype. In addition, chondro-instructive bioactivity could be shown in undifferentiated hMSCs by expression of cartilage-specific factors.

Acknowledgements

We thank Luca Fürst, Nico Oberfranki, Svetlana Belov and Vera Kerling (Faculty of Material Engineering, Nuremberg Institute of Technology Georg Simon Ohm, Nuremberg, Germany) for support in scaffold preparation and Clea Kline for proofreading.

Author´s contributions

Conceptualization, C.G., G.S.-T., methodology, C.G., S.W., A.C., L.F., validation, C.G., G.S.-T., formal analysis, C.G., G.S.-T., S.W., A.L., T.M.W., B.M., investigation, C.G., G.S.-T., writing-original draft preparation C.G., G.S.-T., writing-review and editing, C.G., G.S.-T., S.W., A.L., A.C., T.M.W., K.S.-E., B.M., L.F., M.H., All authors have read and agreed to the published version of the manuscript.

Disclosure of interest

The authors declare that they have no competing interests

Funding

This research was partly supported by a grant of the Staedtler-foundation (to Markus Hornfeck).

References

[1] C.W. Archer, P. Francis-West, The chondrocyte, 35(4) (2003) 401-404.
[2] J. Buckwalter, Articular cartilage injuries, 402 (2002) 21-37.
[3] M. Rahmati, G. Nalesso, A. Mobasheri, M. Mozafari, Aging and osteoarthritis: Central role of the extracellular matrix, Ageing Res Rev 40 (2017) 20-30.
[4] M. Ulrich-Vinther, M.D. Maloney, E.M. Schwarz, R. Rosier, R.J. O'Keefe, Articular cartilage biology, J Am Acad Orthop Surg 11(6) (2003) 421-30.
[5] R.F. Loeser, S.R. Goldring, C.R. Scanzello, M.B.J.A. Goldring, Rheumatism, Osteoarthritis: a disease of the joint as an organ, 64(6) (2012) 1697-1707.
[6] G. Schulze-Tanzil, Intraarticular Ligament Degeneration Is Interrelated with Cartilage and Bone Destruction in Osteoarthritis, Cells 8(9) (2019).
[7] J. Huang, L. Zhao, Y. Fan, L. Liao, P.X. Ma, G. Xiao, D. Chen, The microRNAs miR-204 and miR-211 maintain joint homeostasis and protect against osteoarthritis progression, Nat Commun 10(1) (2019) 2876.
[8] A. Viste, M. Piperno, R. Desmarchelier, S. Grosclaude, B. Moyen, M.H. Fessy, Autologous chondrocyte implantation for traumatic full-thickness cartilage defects of the knee in 14 patients: 6-year functional outcomes, Orthop Traumatol Surg Res 98(7) (2012) 737-43.
[9] M. Brittberg, A. Lindahl, A. Nilsson, C. Ohlsson, O. Isaksson, L. Peterson, Treatment of deep cartilage defects in the knee with autologous chondrocyte transplantation, N Engl J Med 331(14) (1994) 889-95.
[10] M. Brittberg, Autologous chondrocyte transplantation, 367 (1999) S147-S155.
[11] M. Brittberg, Autologous chondrocyte implantation—technique and long-term follow-up, 39(1) (2008) 40-49.
[12] M. Brittberg, D. Recker, J. Ilgenfritz, D.B.F. Saris, S.E.S. Group, Matrix-Applied Characterized Autologous Cultured Chondrocytes Versus Microfracture: Five-Year Follow-up of a Prospective Randomized Trial, Am J Sports Med 46(6) (2018) 1343-1351.

[13] E. Medvedeva, E. Grebenik, S. Gornostaeva, V. Telpuhov, A. Lychagin, P. Timashev, A.J.I.j.o.m.s. Chagin, Repair of damaged articular cartilage: Current approaches and future directions, 19(8) (2018) 2366.
[14] P. Niemeyer, T. Schubert, M. Grebe, A. Hoburg, Treatment Costs of Matrix-Associated Autologous Chondrocyte Implantation Compared With Microfracture: Results of a Matched-Pair Claims Data Analysis on the Treatment of Cartilage Knee Defects in Germany, Orthop J Sports Med 7(12) (2019) 2325967119886583.
[15] M. Brittberg, Cell carriers as the next generation of cell therapy for cartilage repair: a review of the matrix-induced autologous chondrocyte implantation procedure, Am J Sports Med 38(6) (2010) 1259-71.
[16] L. Peterson, H.S. Vasiliadis, M. Brittberg, A. Lindahl, Autologous chondrocyte implantation: a long-term follow-up, Am J Sports Med 38(6) (2010) 1117-24.
[17] P.C. Kreuz, R.H. Kalkreuth, P. Niemeyer, M. Uhl, C. Erggelet, Long-Term Clinical and MRI Results of Matrix-Assisted Autologous Chondrocyte Implantation for Articular Cartilage Defects of the Knee, Cartilage 10(3) (2019) 305-313.
[18] N. Bhardwaj, D. Devi, B.B. Mandal, Tissue-engineered cartilage: the crossroads of biomaterials, cells and stimulating factors, Macromol Biosci 15(2) (2015) 153-82.
[19] B.J. Huang, J.C. Hu, K.A. Athanasiou, Cell-based tissue engineering strategies used in the clinical repair of articular cartilage, Biomaterials 98 (2016) 1-22.
[20] B. Chan, K. Leong, Scaffolding in tissue engineering: general approaches and tissue-specific considerations, 17(4) (2008) 467-479.
[21] D.W. Hutmacher, Scaffolds in tissue engineering bone and cartilage, The biomaterials: Silver jubilee compendium (2000) 175-189.
[22] A.J. Neumann, T. Quinn, S.J. Bryant, Nondestructive evaluation of a new hydrolytically degradable and photo-clickable PEG hydrogel for cartilage tissue engineering, Acta Biomater 39 (2016) 1-11.
[23] A.M. Haaparanta, E. Jarvinen, I.F. Cengiz, V. Ella, H.T. Kokkonen, I. Kiviranta, M. Kellomaki, Preparation and characterization of collagen/PLA, chitosan/PLA, and collagen/chitosan/PLA hybrid scaffolds for cartilage tissue engineering, J Mater Sci Mater Med 25(4) (2014) 1129-36.
[24] D. Barnewitz, M. Endres, I. Krüger, A. Becker, J. Zimmermann, I. Wilke, J. Ringe, M. Sittinger, C. Kaps, Treatment of articular cartilage defects in horses with polymer-based cartilage tissue engineering grafts, Biomaterials 27(14) (2006) 2882-9.
[25] G. Conoscenti, F. Carfì Pavia, A. Ongaro, V. Brucato, C. Goegele, S. Schwarz, A.R. Boccaccini, K. Stoelzel, V. La Carrubba, G. Schulze-Tanzil, Human nasoseptal chondrocytes maintain their differentiated phenotype on PLLA scaffolds produced by thermally induced phase separation and supplemented with bioactive glass 1393, Connect Tissue Res 60(4) (2019) 344-357.
[26] Y. Cai, L. Guo, H. Shen, X. An, H. Jiang, F. Ji, Y. Niu, Degradability, bioactivity, and osteogenesis of biocomposite scaffolds of lithium-containing mesoporous bioglass and mPEG-PLGA-b-PLL copolymer, Int J Nanomedicine 10 (2015) 4125-36.
[27] Z. Terzopoulou, D. Baciu, E. Gounari, T. Steriotis, G. Charalambopoulou, D. Tzetzis, D. Bikiaris, Composite Membranes of Poly(epsilon-caprolactone) with Bisphosphonate-Loaded Bioactive Glasses for Potential Bone Tissue Engineering Applications, Molecules 24(17) (2019).
[28] N. Cui, J. Qian, J. Wang, C. Ji, W. Xu, H. Wang, Preparation, physicochemical properties and biocompatibility of PBLG/PLGA/bioglass composite scaffolds, Mater Sci Eng C Mater Biol Appl 71 (2017) 118-124.
[29] A. Motealleh, S. Eqtesadi, A. Pajares, P. Miranda, Enhancing the mechanical and in vitro performance of robocast bioglass scaffolds by polymeric coatings: Effect of polymer composition, J Mech Behav Biomed Mater 84 (2018) 35-45.
[30] M.N. Rahaman, D.E. Day, B.S. Bal, Q. Fu, S.B. Jung, L.F. Bonewald, A.P. Tomsia, Bioactive glass in tissue engineering, Acta Biomater 7(6) (2011) 2355-73.
[31] M. Khoroushi, F. Keshani, A review of glass-ionomers: From conventional glass-ionomer to bioactive glass-ionomer, Dent Res J (Isfahan) 10(4) (2013) 411-20.
[32] W. Cao, L.L. Hench, Bioactive materials, 22(6) (1996) 493-507.

[33] D.M. Sanders, L.L. Hench, Mechanisms of Glass Corrosion, Journal of the American Ceramic Society 56(7) (1973) 373-377.
[34] I. Ochoa, J.A. Sanz-Herrera, J.M. García-Aznar, M. Doblaré, D.M. Yunos, A.R.J.J.o.b. Boccaccini, Permeability evaluation of 45S5 Bioglass®-based scaffolds for bone tissue engineering, 42(3) (2009) 257-260.
[35] D. Wheeler, K. Stokes, H. Park, J. Hollinger, Evaluation of particulate Bioglass® in a rabbit radius ostectomy model, 35(2) (1997) 249-254.
[36] A. Hoppe, B. Jokic, D. Janackovic, T. Fey, P. Greil, S. Romeis, J. Schmidt, W. Peukert, J. Lao, E. Jallot, A.R. Boccaccini, Cobalt-releasing 1393 bioactive glass-derived scaffolds for bone tissue engineering applications, ACS Appl Mater Interfaces 6(4) (2014) 2865-77.
[37] T.E. Douglas, W. Piwowarczyk, E. Pamula, J. Liskova, D. Schaubroeck, S.C. Leeuwenburgh, G. Brackman, L. Balcaen, R. Detsch, H. Declercq, K. Cholewa-Kowalska, A. Dokupil, V.M. Cuijpers, F. Vanhaecke, R. Cornelissen, T. Coenye, A.R. Boccaccini, P. Dubruel, Injectable self-gelling composites for bone tissue engineering based on gellan gum hydrogel enriched with different bioglasses, Biomed Mater 9(4) (2014) 045014.
[38] I.D. Xynos, A.J. Edgar, L.D. Buttery, L.L. Hench, J.M. Polak, Ionic products of bioactive glass dissolution increase proliferation of human osteoblasts and induce insulin-like growth factor II mRNA expression and protein synthesis, Biochem Biophys Res Commun 276(2) (2000) 461-5.
[39] E. Chrysos, G. Tzovaras, E. Epanomeritakis, J. Tsiaoussis, N. Vrachasotakis, J.S. Vassilakis, E. Xynos, Erythromycin enhances oesophageal motility in patients with gastro-oesophageal reflux, ANZ J Surg 71(2) (2001) 98-102.
[40] T. Jacobs, R. Morent, N. De Geyter, P. Dubruel, C. Leys, Plasma Surface Modification of Biomedical Polymers: Influence on Cell-Material Interaction, Plasma Chem Plasma P 32(5) (2012) 1039-1073.
[41] S.R. Dutta, D. Passi, P. Singh, A. Bhuibhar, Ceramic and non-ceramic hydroxyapatite as a bone graft material: a brief review, Ir J Med Sci 184(1) (2015) 101-6.
[42] N. Ramesh, S.C. Moratti, G.J. Dias, Hydroxyapatite-polymer biocomposites for bone regeneration: A review of current trends, J Biomed Mater Res B Appl Biomater 106(5) (2018) 2046-2057.
[43] E. Suominen, A.J. Aho, E. Vedel, I. Kangasniemi, E. Uusipaikka, A. Yli-Urpo, Subchondral bone and cartilage repair with bioactive glasses, hydroxyapatite, and hydroxyapatite-glass composite, J Biomed Mater Res 32(4) (1996) 543-51.
[44] T. Kumai, N. Yui, K. Yatabe, C. Sasaki, R. Fujii, M. Takenaga, H. Fujiya, H. Niki, K. Yudoh, A novel, self-assembled artificial cartilage-hydroxyapatite conjugate for combined articular cartilage and subchondral bone repair: histopathological analysis of cartilage tissue engineering in rat knee joints, Int J Nanomedicine 14 (2019) 1283-1298.
[45] L. Jia, Z. Duan, D. Fan, Y. Mi, J. Hui, L. Chang, Human-like collagen/nano-hydroxyapatite scaffolds for the culture of chondrocytes, Mater Sci Eng C Mater Biol Appl 33(2) (2013) 727-34.
[46] R. Hill, An alternative view of the degradation of bioglass, 15(13) (1996) 1122-1125.
[47] P. Han, C. Wu, Y. Xiao, The effect of silicate ions on proliferation, osteogenic differentiation and cell signalling pathways (WNT and SHH) of bone marrow stromal cells, Biomater Sci 1(4) (2013) 379-392.
[48] M. Zhang, C. Wu, K. Lin, W. Fan, L. Chen, Y. Xiao, J. Chang, Biological responses of human bone marrow mesenchymal stem cells to Sr-M-Si (M = Zn, Mg) silicate bioceramics, J Biomed Mater Res A 100(11) (2012) 2979-90.
[49] L.F. Bonewald, The amazing osteocyte, J Bone Miner Res 26(2) (2011) 229-38.
[50] S. Nakamura, T. Matsumoto, J. Sasaki, H. Egusa, K.Y. Lee, T. Nakano, T. Sohmura, A. Nakahira, Effect of calcium ion concentrations on osteogenic differentiation and hematopoietic stem cell niche-related protein expression in osteoblasts, Tissue Eng Part A 16(8) (2010) 2467-73.
[51] S. Yamada, A. Obata, H. Maeda, Y. Ota, T. Kasuga, Development of Magnesium and Siloxane-Containing Vaterite and Its Composite Materials for Bone Regeneration, Front Bioeng Biotechnol 3 (2015) 195.

[52] A. Chlanda, P. Oberbek, M. Heljak, E. Kijenska-Gawronska, T. Bolek, M. Gloc, L. John, M. Janeta, M.J. Wozniak, Fabrication, multi-scale characterization and in-vitro evaluation of porous hybrid bioactive glass polymer-coated scaffolds for bone tissue engineering, Mater Sci Eng C Mater Biol Appl 94 (2019) 516-523.
[53] T. Miyazaki, K. Ishikawa, Y. Shirosaki, C. Ohtsuki, Organic-inorganic composites designed for biomedical applications, Biol Pharm Bull 36(11) (2013) 1670-5.
[54] J.J. Blaker, V. Maquet, R. Jerome, A.R. Boccaccini, S.N. Nazhat, Mechanical properties of highly porous PDLLA/Bioglass composite foams as scaffolds for bone tissue engineering, Acta Biomater 1(6) (2005) 643-52.
[55] M. Infanger, P. Kossmehl, M. Shakibaei, G. Schulze-Tanzil, A. Cogoli, S. Faramarzi, J. Bauer, F. Curcio, M. Paul, D. Grimm, Longterm conditions of mimicked weightlessness influences the cytoskeleton in thyroid cells, J Gravit Physiol 11(2) (2004) P169-72.
[56] G. Schulze-Tanzil, Activation and dedifferentiation of chondrocytes: implications in cartilage injury and repair, Ann Anat 191(4) (2009) 325-38.
[57] P. Niemeyer, D. Albrecht, S. Andereya, P. Angele, A. Ateschrang, M. Aurich, M. Baumann, U. Bosch, C. Erggelet, S. Fickert, H. Gebhard, K. Gelse, D. Gunther, A. Hoburg, P. Kasten, T. Kolombe, H. Madry, S. Marlovits, N.M. Meenen, P.E. Muller, U. Noth, J.P. Petersen, M. Pietschmann, W. Richter, B. Rolauffs, K. Rhunau, B. Schewe, A. Steinert, M.R. Steinwachs, G.H. Welsch, W. Zinser, J. Fritz, Autologous chondrocyte implantation (ACI) for cartilage defects of the knee: A guideline by the working group "Clinical Tissue Regeneration" of the German Society of Orthopaedics and Trauma (DGOU), Knee 23(3) (2016) 426-35.
[58] D.G. Phinney, Isolation of mesenchymal stem cells from murine bone marrow by immunodepletion, Mesenchymal Stem Cells, Springer2008, pp. 171-186.
[59] H. Koga, L. Engebretsen, J.E. Brinchmann, T. Muneta, I. Sekiya, Mesenchymal stem cell-based therapy for cartilage repair: a review, Knee Surg Sports Traumatol Arthrosc 17(11) (2009) 1289-97.
[60] J.H. Schefe, K.E. Lehmann, I.R. Buschmann, T. Unger, H. Funke-Kaiser, Quantitative real-time RT-PCR data analysis: current concepts and the novel "gene expression's CT difference" formula, J Mol Med (Berl) 84(11) (2006) 901-10.
[61] J. Iwasa, L. Engebretsen, Y. Shima, M. Ochi, Clinical application of scaffolds for cartilage tissue engineering, Knee Surg Sports Traumatol Arthrosc 17(6) (2009) 561-77.
[62] P. Behrens, T. Bitter, B. Kurz, M. Russlies, Matrix-associated autologous chondrocyte transplantation/implantation (MACT/MACI)--5-year follow-up, Knee 13(3) (2006) 194-202.
[63] C.G. Pfeifer, A. Berner, M. Koch, W. Krutsch, R. Kujat, P. Angele, M. Nerlich, J. Zellner, Higher Ratios of Hyaluronic Acid Enhance Chondrogenic Differentiation of Human MSCs in a Hyaluronic Acid-Gelatin Composite Scaffold, Materials (Basel) 9(5) (2016).
[64] M. Falah, G. Nielsenberg, M. Soudry, M. Hayden, G. Volpin, Treatment of articular cartilage lesions of the knee, Int Orthop 34(5) (2010) 621-30.
[65] L. Gao, P. Orth, M. Cucchiarini, H. Madry, Effects of solid acellular type-I/III collagen biomaterials on in vitro and in vivo chondrogenesis of mesenchymal stem cells, Expert Rev Med Devices 14(9) (2017) 717-732.
[66] J.F. Guo, G.W. Jourdian, D.K. MacCallum, Culture and growth characteristics of chondrocytes encapsulated in alginate beads, Connect Tissue Res 19(2-4) (1989) 277-97.
[67] X. Li, S. Chen, J. Li, X. Wang, J. Zhang, N. Kawazoe, G. Chen, 3D Culture of Chondrocytes in Gelatin Hydrogels with Different Stiffness, Polymers (Basel) 8(8) (2016).
[68] M.M. Caron, P.J. Emans, M.M. Coolsen, L. Voss, D.A. Surtel, A. Cremers, L.W. van Rhijn, T.J. Welting, Redifferentiation of dedifferentiated human articular chondrocytes: comparison of 2D and 3D cultures, Osteoarthritis Cartilage 20(10) (2012) 1170-8.
[69] G. Conoscenti, T. Schneider, K. Stoelzel, F. Carfi Pavia, V. Brucato, C. Goegele, V. La Carrubba, G. Schulze-Tanzil, PLLA scaffolds produced by thermally induced phase separation (TIPS) allow human chondrocyte growth and extracellular matrix formation dependent on pore size, Mater Sci Eng C Mater Biol Appl 80 (2017) 449-459.
[70] S.H. Oh, T.H. Kim, G.I. Im, J.H. Lee, Investigation of pore size effect on chondrogenic differentiation of adipose stem cells using a pore size gradient scaffold, Biomacromolecules 11(8) (2010) 1948-55.

[71] P.J. Emans, E.J. Jansen, D. van Iersel, T.J. Welting, T.B. Woodfield, S.K. Bulstra, J. Riesle, L.W. van Rhijn, R. Kuijer, Tissue-engineered constructs: the effect of scaffold architecture in osteochondral repair, J Tissue Eng Regen Med 7(9) (2013) 751-6.
[72] M.J. Gupte, W.B. Swanson, J. Hu, X. Jin, H. Ma, Z. Zhang, Z. Liu, K. Feng, G. Feng, G. Xiao, N. Hatch, Y. Mishina, P.X. Ma, Pore size directs bone marrow stromal cell fate and tissue regeneration in nanofibrous macroporous scaffolds by mediating vascularization, Acta Biomater 82 (2018) 1-11.
[73] F. Zhang, Q. He, W.P. Tsang, W.T. Garvey, W.Y. Chan, C. Wan, Insulin exerts direct, IGF-1 independent actions in growth plate chondrocytes, Bone Res 2 (2014) 14012.
[74] R.A. Stockwell, Biology of cartilage cells, CUP Archive1979.
[75] J. Ge, L. Guo, S. Wang, Y. Zhang, T. Cai, R.C. Zhao, Y. Wu, The size of mesenchymal stem cells is a significant cause of vascular obstructions and stroke, Stem Cell Rev Rep 10(2) (2014) 295-303.
[76] K. Stölzel, G. Schulze-Tanzil, H. Olze, S. Schwarz, E.M. Feldmann, N. Rotter, Immortalised human mesenchymal stem cells undergo chondrogenic differentiation in alginate and PGA/PLLA scaffolds, Cell Tissue Bank 16(1) (2015) 159-70.
[77] J. Ajita, S. Saravanan, N. Selvamurugan, Effect of size of bioactive glass nanoparticles on mesenchymal stem cell proliferation for dental and orthopedic applications, Mater Sci Eng C Mater Biol Appl 53 (2015) 142-9.
[78] T. Sun, M. Wang, Y. Shao, L. Wang, Y. Zhu, The Effect and Osteoblast Signaling Response of Trace Silicon Doping Hydroxyapatite, Biol Trace Elem Res 181(1) (2018) 82-94.
[79] W.C. Vrouwenvelder, C.G. Groot, K. de Groot, Better histology and biochemistry for osteoblasts cultured on titanium-doped bioactive glass: bioglass 45S5 compared with iron-, titanium-, fluorine- and boron-containing bioactive glasses, Biomaterials 15(2) (1994) 97-106.
[80] A. Asselin, S. Hattar, M. Oboeuf, D. Greenspan, A. Berdal, J.M. Sautier, The modulation of tissue-specific gene expression in rat nasal chondrocyte cultures by bioactive glasses, Biomaterials 25(25) (2004) 5621-30.
[81] A.B. Cook, A.W. Seifert, Beryllium nitrate inhibits fibroblast migration to disrupt epimorphic regeneration, Development 143(19) (2016) 3491-3505.
[82] S.S. Coates, B.E. Lehnert, S. Sharma, S.M. Kindell, R.K. Gary, Beryllium induces premature senescence in human fibroblasts, J Pharmacol Exp Ther 322(1) (2007) 70-9.
[83] H. Zreiqat, C.R. Howlett, A. Zannettino, P. Evans, G. Schulze-Tanzil, C. Knabe, M. Shakibaei, Mechanisms of magnesium-stimulated adhesion of osteoblastic cells to commonly used orthopaedic implants, J Biomed Mater Res 62(2) (2002) 175-84.
[84] B.S. Kim, J.S. Kim, Y.M. Park, B.Y. Choi, J. Lee, Mg ion implantation on SLA-treated titanium surface and its effects on the behavior of mesenchymal stem cell, Mater Sci Eng C Mater Biol Appl 33(3) (2013) 1554-60.
[85] W. Zhao, J. Chang, J. Wang, W. Zhai, Z. Wang, In vitro bioactivity of novel tricalcium silicate ceramics, J Mater Sci Mater Med 18(5) (2007) 917-23.
[86] D. Laurencin, N. Almora-Barrios, N.H. de Leeuw, C. Gervais, C. Bonhomme, F. Mauri, W. Chrzanowski, J.C. Knowles, R.J. Newport, A. Wong, Z. Gan, M.E. Smith, Magnesium incorporation into hydroxyapatite, Biomaterials 32(7) (2011) 1826-37.
[87] S. Samavedi, A.R. Whittington, A.S. Goldstein, Calcium phosphate ceramics in bone tissue engineering: a review of properties and their influence on cell behavior, Acta Biomater 9(9) (2013) 8037-45.
[88] J. Lacroix, J. Lao, J.M. Nedelec, E. Jallot, Micro PIXE-RBS for the study of Sr release at bioactive glass scaffolds/biological medium interface, Nucl Instrum Meth B 306 (2013) 153-157.
[89] S.K. Arepalli, H. Tripathi, V.K. Vyas, S. Jain, S.K. Suman, R. Pyare, S.P. Singh, Influence of barium substitution on bioactivity, thermal and physico-mechanical properties of bioactive glass, Mater Sci Eng C Mater Biol Appl 49 (2015) 549-559.
[90] S. Luo, Q. Shi, W. Li, W. Wu, Z. Zha, ITGB1 promotes the chondrogenic differentiation of human adipose-derived mesenchymal stem cells by activating the ERK signaling, J Mol Histol 51(6) (2020) 729-739.

[91] Y. Wang, Y. Xiao, S. Long, Y. Fan, X. Zhang, Role of N-Cadherin in a Niche-Mimicking Microenvironment for Chondrogenesis of Mesenchymal Stem Cells In Vitro, ACS Biomater Sci Eng 6(6) (2020) 3491-3501.
[92] Y. Yang, Y. Liu, Z. Lin, H. Shen, C. Lucas, B. Kuang, R.S. Tuan, H. Lin, Condensation-Driven Chondrogenesis of Human Mesenchymal Stem Cells within Their Own Extracellular Matrix: Formation of Cartilage with Low Hypertrophy and Physiologically Relevant Mechanical Properties, Adv Biosyst 3(12) (2019) e1900229.
[93] A. Mobasheri, S.D. Carter, P. Martin-Vasallo, M. Shakibaei, Integrins and stretch activated ion channels; putative components of functional cell surface mechanoreceptors in articular chondrocytes, Cell Biol Int 26(1) (2002) 1-18.
[94] S.L. Vega, M. Kwon, R.L. Mauck, J.A. Burdick, Single Cell Imaging to Probe Mesenchymal Stem Cell N-Cadherin Mediated Signaling within Hydrogels, Ann Biomed Eng 44(6) (2016) 1921-30.
[95] S.D. Bird, Calcium mediates cell shape change in human peritoneal mesothelial cells, Cell Calcium 72 (2018) 116-126.
[96] F. Westhauser, M. Karadjian, C. Essers, A.S. Senger, S. Hagmann, G. Schmidmaier, A. Moghaddam, Osteogenic differentiation of mesenchymal stem cells is enhanced in a 45S5-supplemented beta-TCP composite scaffold: an in-vitro comparison of Vitoss and Vitoss BA, PLoS One 14(2) (2019) e0212799.
[97] J. Wu, K. Xue, H. Li, J. Sun, K. Liu, Improvement of PHBV scaffolds with bioglass for cartilage tissue engineering, PLoS One 8(8) (2013) e71563.
[98] H. Oonishi, L.L. Hench, J. Wilson, F. Sugihara, E. Tsuji, M. Matsuura, S. Kin, T. Yamamoto, S. Mizokawa, Quantitative comparison of bone growth behavior in granules of Bioglass, A-W glass-ceramic, and hydroxyapatite, J Biomed Mater Res 51(1) (2000) 37-46.
[99] S. Gorodzha, T.E. Douglas, S.K. Samal, R. Detsch, K. Cholewa-Kowalska, K. Braeckmans, A.R. Boccaccini, A.G. Skirtach, V. Weinhardt, T. Baumbach, M.A. Surmeneva, R.A. Surmenev, High-resolution synchrotron X-ray analysis of bioglass-enriched hydrogels, J Biomed Mater Res A 104(5) (2016) 1194-201.
[100] I.A. Silver, J. Deas, M. Erecinska, Interactions of bioactive glasses with osteoblasts in vitro: effects of 45S5 Bioglass, and 58S and 77S bioactive glasses on metabolism, intracellular ion concentrations and cell viability, Biomaterials 22(2) (2001) 175-85.
[101] S. Grad, L. Kupcsik, K. Gorna, S. Gogolewski, M. Alini, The use of biodegradable polyurethane scaffolds for cartilage tissue engineering: potential and limitations, Biomaterials 24(28) (2003) 5163-71.
[102] P.Y. Wang, H.H. Chow, J.Y. Lai, H.L. Liu, W.B. Tsai, Dynamic compression modulates chondrocyte proliferation and matrix biosynthesis in chitosan/gelatin scaffolds, J Biomed Mater Res B Appl Biomater 91(1) (2009) 143-52.
[103] P.S.P. Poh, D.W. Hutmacher, B.M. Holzapfel, A.K. Solanki, M.M. Stevens, M.A. Woodruff, In vitro and in vivo bone formation potential of surface calcium phosphate-coated polycaprolactone and polycaprolactone/bioactive glass composite scaffolds, Acta Biomater 30 (2016) 319-333.
[104] N. Cheng, Y. Wang, Y. Zhang, B. Shi, The osteogenic potential of mesoporous bioglasses/silk and non-mesoporous bioglasses/silk scaffolds in ovariectomized rats: in vitro and in vivo evaluation, PLoS One 8(11) (2013) e81014.
[105] N. Sawatjui, T. Limpaiboon, K. Schrobback, T. Klein, Biomimetic scaffolds and dynamic compression enhance the properties of chondrocyte- and MSC-based tissue-engineered cartilage, J Tissue Eng Regen Med 12(5) (2018) 1220-1229.
[106] Q. Zhang, H.X. Lu, N. Kawazoe, G.P. Chen, Preparation of collagen scaffolds with controlled pore structures and improved mechanical property for cartilage tissue engineering, J Bioact Compat Pol 28(5) (2013) 426-438.
[107] Y. Agirdil, The growth plate: a physiologic overview, EFORT Open Rev 5(8) (2020) 498-507.
[108] F.H. Chen, K.T. Rousche, R.S. Tuan, Technology Insight: adult stem cells in cartilage regeneration and tissue engineering, Nat Clin Pract Rheumatol 2(7) (2006) 373-82.

[109] M. Locker, O. Kellermann, M. Boucquey, H. Khun, M. Huerre, A. Poliard, Paracrine and autocrine signals promoting full chondrogenic differentiation of a mesoblastic cell line, J Bone Miner Res 19(1) (2004) 100-10.
[110] D.A. Foyt, D.K. Taheem, S.A. Ferreira, M.D.A. Norman, J. Petzold, G. Jell, A.E. Grigoriadis, E. Gentleman, Hypoxia impacts human MSC response to substrate stiffness during chondrogenic differentiation, Acta Biomater 89 (2019) 73-83.
[111] T. Re'em, Y. Kaminer-Israeli, E. Ruvinov, S. Cohen, Chondrogenesis of hMSC in affinity-bound TGF-beta scaffolds, Biomaterials 33(3) (2012) 751-61.
[112] C. Kiani, L. Chen, Y.J. Wu, A.J. Yee, B.B. Yang, Structure and function of aggrecan, Cell Res 12(1) (2002) 19-32.
[113] J.S. Mort, Y. Geng, W.D. Fisher, P.J. Roughley, Aggrecan heterogeneity in articular cartilage from patients with osteoarthritis, BMC Musculoskelet Disord 17 (2016) 89.
[114] H.M. Ávila, S. Schwarz, N. Rotter, P. Gatenholm, 3D bioprinting of human chondrocyte-laden nanocellulose hydrogels for patient-specific auricular cartilage regeneration, Bioprinting 1 (2016) 22-35.
[115] M.H. Beigi, A. Atefi, H.R. Ghanaei, S. Labbaf, F. Ejeian, M.H. Nasr-Esfahani, Activated platelet-rich plasma improves cartilage regeneration using adipose stem cells encapsulated in a 3D alginate scaffold, J Tissue Eng Regen Med 12(6) (2018) 1327-1338.
[116] M. Zhou, D. Yu, Cartilage tissue engineering using PHBV and PHBV/Bioglass scaffolds, Mol Med Rep 10(1) (2014) 508-14.
[117] B. Mikic, A.L. Isenstein, A. Chhabra, Mechanical modulation of cartilage structure and function during embryogenesis in the chick, Ann Biomed Eng 32(1) (2004) 18-25.
[118] K. Matsumoto, N. Kamiya, K. Suwan, F. Atsumi, K. Shimizu, T. Shinomura, Y. Yamada, K. Kimata, H. Watanabe, Identification and characterization of versican/PG-M aggregates in cartilage, J Biol Chem 281(26) (2006) 18257-63.
[119] M.S. Muttigi, I. Han, H.K. Park, H. Park, S.H. Lee, Matrilin-3 Role in Cartilage Development and Osteoarthritis, Int J Mol Sci 17(4) (2016).
[120] R. Kuijer, R.J. van de Stadt, M.H. de Koning, G.P. van Kampen, J.K. van der Korst, Influence of cartilage proteoglycans on type II collagen fibrillogenesis, Connect Tissue Res 17(2) (1988) 83-97.
[121] D.T. Yamaguchi, J.T. Huang, D. Ma, Regulation of gap junction intercellular communication by pH in MC3T3-E1 osteoblastic cells, J Bone Miner Res 10(12) (1995) 1891-9.
[122] R.A. Johnson, Changes in pH sensitivity of adenylate cyclase specifically induced by fluoride and vanadate, Arch Biochem Biophys 218(1) (1982) 68-76.

Declaration of interest

The authors declare that they have no competing interests and no conflict of interest.

They confirm that this manuscript has not been published previously. It is not under consideration for publication elsewhere, and, if accepted, it will not be published elsewhere in the same form, in English or in any other language.

As the corresponding author confirm the above statements on behalf of the coauthors

With kind regards

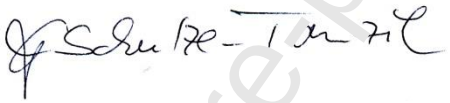

Univ.-Prof. Dr. Gundula Schulze-Tanzil

Graphical abstract